

ENSEMBLE TIMESTEPPING ALGORITHMS FOR NATURAL CONVECTION

J. A. FIORDILINO* AND S. KHANKAN*

Abstract. This paper presents two algorithms for calculating an ensemble of solutions to laminar natural convection problems. The ensemble average is the most likely temperature distribution and its variance gives an estimate of prediction reliability. Solutions are calculated by solving two coupled linear systems, each involving a shared coefficient matrix, for multiple right-hand sides at each timestep. Storage requirements and computational costs to solve the system are thereby reduced. Stability and convergence of the method are proven under a timestep condition involving fluctuations. A series of numerical tests, including predictability horizons, are provided which confirm the theoretical analyses and illustrate uses of ensemble simulations.

1. Introduction. Ensemble calculations are essential in predictions of the most likely outcome of systems with uncertain data, e.g., weather forecasting [12], ocean modeling [14], turbulence [11], etc. Ensemble simulations classically involve J sequential, fine mesh runs or J parallel, coarse mesh runs of a given code. This leads to a competition between ensemble size and mesh density. We develop linearly implicit timestepping methods with shared coefficient matrices to address this issue. For such methods, it is more efficient in both storage and solution time to solve J linear systems with a shared coefficient matrix than with J different matrices.

Prediction of thermal profiles is essential in many applications [1, 7, 16, 17]. Herein, we extend [6] from isothermal flows to temperature dependent natural convection. We consider two natural convection problems enclosed in mediums with: **non-zero wall thickness** [3] and **zero wall thickness**; Figure 1 illustrates a typical setup. The latter problem is often utilized as a thin wall approximation.

Consider the **Thick wall problem**. Let $\Omega_f \subset \Omega$ be polyhedral domains in $\mathbb{R}^d (d = 2, 3)$ with boundaries $\partial\Omega_f$ and $\partial\Omega$, respectively, such that $\text{dist}(\partial\Omega_f, \partial\Omega) > 0$. The boundary $\partial\Omega$ is partitioned such that $\partial\Omega = \Gamma_1 \cup \Gamma_2$ with $\Gamma_1 \cap \Gamma_2 = \emptyset$ and $|\Gamma_1| > 0$. Given $u(x, 0; \omega_j) = u^0(x; \omega_j)$ and $T(x, 0; \omega_j) = T^0(x; \omega_j)$ for $j = 1, 2, \dots, J$, let $u(x, t; \omega_j) : \Omega \times (0, t^*] \rightarrow \mathbb{R}^d$, $p(x, t; \omega_j) : \Omega \times (0, t^*] \rightarrow \mathbb{R}$, and $T(x, t; \omega_j) : \Omega \times (0, t^*] \rightarrow \mathbb{R}$ satisfy

$$\begin{aligned} (1) \quad & u_t + u \cdot \nabla u - Pr \Delta u + \nabla p = Pr Ra \gamma T + f \text{ in } \Omega_f, \\ (2) \quad & \nabla \cdot u = 0 \text{ in } \Omega_f, \\ (3) \quad & T_t + u \cdot \nabla T - \nabla \cdot (\kappa \nabla T) = g \text{ in } \Omega, \\ (4) \quad & u = 0 \text{ on } \partial\Omega_f, \quad u = 0 \text{ in } \Omega - \Omega_f, \quad T = 0 \text{ on } \Gamma_1 \text{ and } n \cdot \nabla T = 0 \text{ on } \Gamma_2. \end{aligned}$$

Here n denotes the usual outward normal, γ denotes the unit vector in the direction of gravity, Pr is the Prandtl number, Ra is the Rayleigh number, and $\kappa = \kappa_f$ in Ω_f and $\kappa = \kappa_s$ in $\Omega - \Omega_f$ is the thermal conductivity of the fluid or solid medium. Further, f and g are the body force and heat source, respectively.

Let $\langle u \rangle^n := \frac{1}{J} \sum_{j=1}^J u^n$ and $u'^n = u^n - \langle u \rangle^n$. To present the idea, suppress the spatial discretization for the moment. We apply an implicit-explicit time-discretization to the system (1) - (4), while keeping the coefficient matrix independent of the ensemble members. This leads to the following timestepping method:

$$\begin{aligned} (5) \quad & \frac{u^{n+1} - u^n}{\Delta t} + \langle u \rangle^n \cdot \nabla u^{n+1} + u'^n \cdot \nabla u^n - Pr \Delta u^{n+1} + \nabla p^{n+1} = Pr Ra \gamma T^{n+1} + f^{n+1}, \\ (6) \quad & \nabla \cdot u^{n+1} = 0, \\ (7) \quad & \frac{T^{n+1} - T^n}{\Delta t} + \langle u \rangle^n \cdot \nabla T^{n+1} + u'^n \cdot \nabla T^n - \kappa \Delta T^{n+1} = g^{n+1}, \end{aligned}$$

Consider the **Thin wall problem**. The main difference is a “ u_1 ” term on the r.h.s of the temperature equation (10) absent in (3). This apparently small difference in the model produces a significant difference in the stability of the approximate solution. In particular, a discrete Gronwall inequality is used which allows

*University of Pittsburgh, Department of Mathematics, Pittsburgh, PA 15260

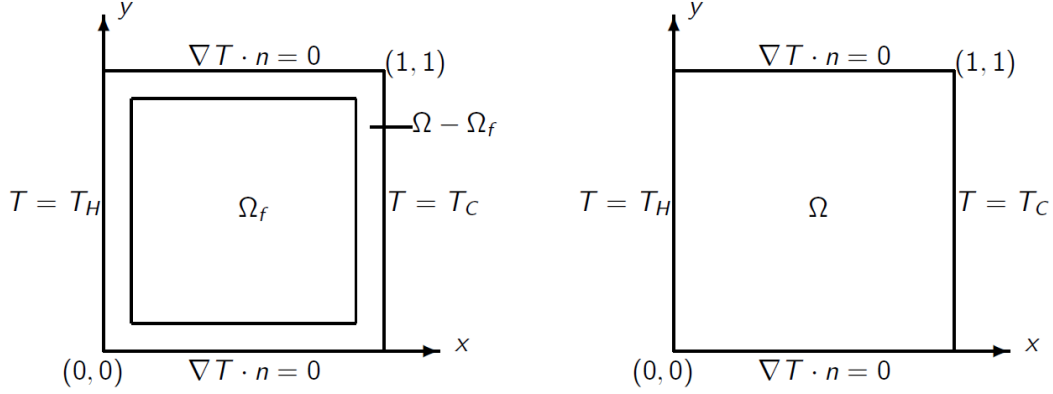


Fig. 1: Domain and boundary conditions for (a) thick walled (b) thin walled double pane window problem benchmark.

for the loss of long-time stability; see Section 4 below. Consider:

$$(8) \quad u_t + u \cdot \nabla u - Pr \Delta u + \nabla p = Pr Ra \gamma T + f \text{ in } \Omega,$$

$$(9) \quad \nabla \cdot u = 0 \text{ in } \Omega,$$

$$(10) \quad T_t + u \cdot \nabla T - \nabla \cdot (\kappa \nabla T) = u_1 + g \text{ in } \Omega,$$

$$(11) \quad u = 0 \text{ on } \partial\Omega, \quad T = 0 \text{ on } \Gamma_1, \quad n \cdot \nabla T = 0 \text{ on } \Gamma_2,$$

where u_1 is the first component of the velocity. If we again momentarily disregard the spatial discretization, our timestepping method can be written as:

$$(12) \quad \frac{u^{n+1} - u^n}{\Delta t} + \langle u \rangle^n \cdot \nabla u^{n+1} + u'^n \cdot \nabla u^n - Pr \Delta u^{n+1} + \nabla p^{n+1} = Pr Ra \gamma T^n + f^{n+1},$$

$$(13) \quad \nabla \cdot u^{n+1} = 0,$$

$$(14) \quad \frac{T^{n+1} - T^n}{\Delta t} + \langle u \rangle^n \cdot \nabla T^{n+1} + u'^n \cdot \nabla T^n - \kappa \Delta T^{n+1} = u_1^n + g^{n+1},$$

By lagging both u' and the coupling terms in the method, the fluid and thermal problems uncouple and each sub-problem has a shared coefficient matrix for all ensemble members.

Remark: The formulation (5) - (7) arises, e.g., in the study of natural convection within a unit square or cubic enclosure with a pair of differentially heated vertical walls. In particular, the temperature distribution is decomposed into $\theta(x, t) = T(x, t) + \phi(x)$, where $\phi(x) = 1 - x_1$ is the linear conduction profile and $T(x, t)$ satisfies homogeneous boundary conditions on the corresponding pair of vertical walls.

In Section 2, we collect necessary mathematical tools. In Section 3, we present algorithms based on (5) - (7) and (12) - (14). Stability and error analyses follow in Section 4. We end with numerical experiments and conclusions in Sections 5 and 6. In particular, two stable, convergent ensemble algorithms are presented. These algorithms can be used to efficiently compute an ensemble of solutions to (1) - (4) and (8) - (11) and estimate predictability horizons. The ensemble average is shown to produce a better estimate of the energy in the system, for a test problem, than any member of the ensemble.

2. Mathematical Preliminaries. The $L^2(\Omega)$ inner product is (\cdot, \cdot) and the induced norm is $\|\cdot\|$. Define the Hilbert spaces,

$$X := H_0^1(\Omega)^d = \{v \in H^1(\Omega)^d : v = 0 \text{ on } \partial\Omega\}, \quad Q := L_0^2(\Omega) = \{q \in L^2(\Omega) : \int_{\Omega} q dx = 0\},$$

$$W := \{S \in H^1(\Omega) : S = 0 \text{ on } \Gamma_1\}, \quad V := \{v \in X : (q, \nabla \cdot v) = 0 \forall q \in Q\}.$$

The explicitly skew-symmetric trilinear forms are denoted:

$$\begin{aligned} b(u, v, w) &= \frac{1}{2}(u \cdot \nabla v, w) - \frac{1}{2}(u \cdot \nabla w, v) \quad \forall u, v, w \in X, \\ b^*(u, T, S) &= \frac{1}{2}(u \cdot \nabla T, S) - \frac{1}{2}(u \cdot \nabla S, T) \quad \forall u \in X, \forall T, S \in W. \end{aligned}$$

They enjoy the following continuity results and properties.

LEMMA 1. *There are constants C_1, C_2, C_3, C_4, C_5 , and C_6 such that for all $u, v, w \in X$ and $T, S \in W$, $b(u, v, w)$ and $b^*(u, T, S)$ satisfy*

$$\begin{aligned} b(u, v, w) &= \int_{\Omega} u \cdot \nabla v \cdot w dx + \frac{1}{2} \int_{\Omega} (\nabla \cdot u) v \cdot w dx, \\ b^*(u, T, S) &= \int_{\Omega} u \cdot \nabla T S dx + \frac{1}{2} \int_{\Omega} (\nabla \cdot u) T S dx, \\ b(u, v, w) &\leq C_1 \|\nabla u\| \|\nabla v\| \|\nabla w\|, \\ b(u, v, w) &\leq C_2 \sqrt{\|u\| \|\nabla u\|} \|\nabla v\| \|\nabla w\|, \\ b^*(u, T, S) &\leq C_3 \|\nabla u\| \|\nabla T\| \|\nabla S\|, \\ b^*(u, T, S) &\leq C_4 \sqrt{\|u\| \|\nabla u\|} \|\nabla T\| \|\nabla S\|, \\ b(u, v, w) &\leq C_5 \|\nabla u\| \|\nabla v\| \sqrt{\|w\| \|\nabla w\|}, \\ b^*(u, T, S) &\leq C_6 \|\nabla u\| \|\nabla T\| \sqrt{\|S\| \|\nabla S\|}. \end{aligned}$$

Proof. The proof of the first two identities is a calculation. The next four results follow from applications of Hölder and Sobolev embedding inequalities; see Lemma 2.2 on p. 2044 of [13]. We will prove the last two results for $d = 3$; for $d = 2$ they are improvable. For all $u, v, w \in X$,

$$\begin{aligned} |(u \cdot \nabla v, w)| &\leq C \|u\|_{L^6} \|\nabla v\| \|w\|_{L^3} \\ &\leq C \|\nabla u\| \|\nabla v\| \sqrt{\|w\| \|\nabla w\|}, \end{aligned}$$

where Hölder, Ladyzhenskaya and Gagliardo-Nirenberg inequalities were used, respectively. Using the above result and inequalities and the first identity in Lemma 1,

$$\begin{aligned} |b(u, v, w)| &= |(u \cdot \nabla v, w) + \frac{1}{2} \int_{\Omega} (\nabla \cdot u) v \cdot w dx| \\ &\leq |(u \cdot \nabla v, w)| + |\frac{1}{2} \int_{\Omega} (\nabla \cdot u) v \cdot w dx| \\ &\leq C \|\nabla u\| \|\nabla v\| \sqrt{\|w\| \|\nabla w\|} + C \|\nabla \cdot u\| \|v\|_{L^6} \|w\|_{L^3} \\ &\leq C \|\nabla u\| \|\nabla v\| \sqrt{\|w\| \|\nabla w\|} + C \|\nabla u\| \|\nabla v\| \sqrt{\|w\| \|\nabla w\|} \\ &\leq C \|\nabla u\| \|\nabla v\| \sqrt{\|w\| \|\nabla w\|}. \end{aligned}$$

In similar fashion, there is a $C = C(\Omega)$ such that

$$\begin{aligned} |b^*(u, T, S)| &\leq |(u \cdot \nabla T, S) + \frac{1}{2} \int_{\Omega} (\nabla \cdot u) T S dx| \\ &\leq C \|\nabla u\| \|\nabla T\| \sqrt{\|S\| \|\nabla S\|} + C \|\nabla \cdot u\| \|T\|_{L^6} \|S\|_{L^3} \\ &\leq C \|\nabla u\| \|\nabla T\| \sqrt{\|S\| \|\nabla S\|} + C \|\nabla u\| \|\nabla T\| \sqrt{\|S\| \|\nabla S\|} \\ &\leq C \|\nabla u\| \|\nabla T\| \sqrt{\|S\| \|\nabla S\|}. \end{aligned}$$

□

The weak formulation of system (1) - (4) is: Find $u : [0, t^*] \rightarrow X$, $p : [0, t^*] \rightarrow Q$, $T : [0, t^*] \rightarrow W$ for a.e. $t \in (0, t^*]$ satisfying for $j = 1, \dots, J$:

$$(15) \quad (u_t, v) + b(u, u, v) + Pr(\nabla u, \nabla v) - (p, \nabla \cdot v) = PrRa(\gamma T, v) + (f, v) \quad \forall v \in X,$$

$$(16) \quad (q, \nabla \cdot u) = 0 \quad \forall q \in Q,$$

$$(17) \quad (T_t, S) + b^*(u, T, S) + \kappa(\nabla T, \nabla S) = (g, S) \quad \forall S \in W.$$

Similarly, the weak formulation of system (8) - (11) is: Find $u : [0, t^*] \rightarrow X$, $p : [0, t^*] \rightarrow Q$, $T : [0, t^*] \rightarrow W$ for a.e. $t \in (0, t^*]$ satisfying for $j = 1, \dots, J$:

$$(18) \quad (u_t, v) + b(u, u, v) + Pr(\nabla u, \nabla v) - (p, \nabla \cdot v) = PrRa(\gamma T, v) + (f, v) \quad \forall v \in X,$$

$$(19) \quad (q, \nabla \cdot u) = 0 \quad \forall q \in Q,$$

$$(20) \quad (T_t, S) + b^*(u, T, S) + \kappa(\nabla T, \nabla S) = (u_1, S) + (g, S) \quad \forall S \in W.$$

2.1. Finite Element Preliminaries. Consider a regular, quasi-uniform mesh $\Omega_h = \{K\}$ of Ω with maximum triangle diameter length h . Further, for the system (1) - (4), suppose that $\partial\Omega_f$ and $\partial\Omega - \partial\Omega_f$ lie along the meshlines of the triangulation of Ω . Let $X_h \subset X$, $Q_h \subset Q$, and $W_h \subset W$ be conforming finite element spaces consisting of continuous piecewise polynomials of degrees j , l , and j , respectively. Moreover, assume they satisfy the following approximation properties $\forall 1 \leq j, l \leq k, m$:

$$(21) \quad \inf_{v_h \in X_h} \left\{ \|u - v_h\| + h \|\nabla(u - v_h)\| \right\} \leq Ch^{k+1} |u|_{k+1},$$

$$(22) \quad \inf_{q_h \in Q_h} \|p - q_h\| \leq Ch^m |p|_m,$$

$$(23) \quad \inf_{S_h \in W_h} \left\{ \|T - S_h\| + h \|\nabla(T - S_h)\| \right\} \leq Ch^{k+1} |T|_{k+1},$$

for all $u \in X \cap H^{k+1}(\Omega)^d$, $p \in Q \cap H^m(\Omega)$, and $T \in W \cap H^{k+1}(\Omega)$. Furthermore, we consider those spaces for which the discrete inf-sup condition is satisfied,

$$(24) \quad \inf_{q_h \in Q_h} \sup_{v_h \in X_h} \frac{(q_h, \nabla \cdot v_h)}{\|q_h\| \|\nabla v_h\|} \geq \beta > 0,$$

where β is independent of h . The space of discretely divergence free functions is defined by

$$V_h := \{v_h \in X_h : (q_h, \nabla \cdot v_h) = 0, \forall q_h \in Q_h\}.$$

The space V_h^* , dual to V_h , is endowed with the following dual norm

$$\|w\|_{V_h^*} := \sup_{v_h \in V_h} \frac{(w, v_h)}{\|\nabla v_h\|}.$$

The discrete inf-sup condition implies that we may approximate functions in V well by functions in V_h ,

LEMMA 2. Suppose the discrete inf-sup condition (24) holds, then for any $v \in V$

$$\inf_{v_h \in V_h} \|\nabla(v - v_h)\| \leq C(\beta) \inf_{v_h \in X_h} \|\nabla(v - v_h)\|.$$

Proof. See Chapter 2, Theorem 1.1 on p. 59 of [8]. □

We will also assume that the mesh and finite element spaces satisfy the standard inverse inequality [5]:

$$\|\nabla \chi_{1,2}\| \leq C_{inv,1,2}(\alpha_{min}) h^{-1} \|\chi_{1,2}\| \quad \forall \chi_1 \in X_h, \quad \forall \chi_2 \in W_h,$$

where α_{min} denotes the minimum angle in the triangulation. A discrete Gronwall inequality will play a role in the upcoming analysis.

LEMMA 3. (Discrete Gronwall Lemma). Let Δt , H , a_n , b_n , c_n , and d_n be finite nonnegative numbers for $n \geq 0$ such that for $N \geq 1$

$$a_N + \Delta t \sum_0^N b_n \leq \Delta t \sum_0^{N-1} d_n a_n + \Delta t \sum_0^N c_n + H,$$

then for all $\Delta t > 0$ and $N \geq 1$

$$a_N + \Delta t \sum_0^N b_n \leq \exp(\Delta t \sum_0^{N-1} d_n) (\Delta t \sum_0^N c_n + H).$$

Proof. See Lemma 5.1 on p. 369 of [10]. □

The discrete time analysis will utilize the following norms $\forall 1 \leq k \leq \infty$:

$$\|v\|_{\infty, k} := \max_{0 \leq n \leq N} \|v^n\|_k, \quad \|v\|_{p, k} := \left(\Delta t \sum_{n=0}^N \|v^n\|_k^p \right)^{1/p}.$$

3. Numerical Scheme. Denote the fully discrete solutions by u_h^n , p_h^n , and T_h^n at time levels $t^n = n\Delta t$, $n = 0, 1, \dots, N$, and $t^* = N\Delta t$. Given $(u_h^n, p_h^n, T_h^n) \in (X_h, Q_h, W_h)$, find $(u_h^{n+1}, p_h^{n+1}, T_h^{n+1}) \in (X_h, Q_h, W_h)$ satisfying, for every $n = 0, 1, \dots, N$, the fully discrete approximation of the **Thick wall problem**:

$$(25) \quad \left(\frac{u_h^{n+1} - u_h^n}{\Delta t}, v_h \right) + b(< u_h >^n, u_h^{n+1}, v_h) + b(u_h'^n, u_h^n, v_h) + Pr(\nabla u_h^{n+1}, \nabla v_h) - (p_h^{n+1}, \nabla \cdot v_h) \\ = PrRa(\gamma T_h^{n+1}, v_h) + (f^{n+1}, v_h) \quad \forall v_h \in X_h,$$

$$(26) \quad (q_h, \nabla \cdot u_h^{n+1}) = 0 \quad \forall q_h \in Q_h,$$

$$(27) \quad \left(\frac{T_h^{n+1} - T_h^n}{\Delta t}, S_h \right) + b^*(< u_h >^n, T_h^{n+1}, S_h) + b^*(u_h'^n, T_h^n, S_h) + \kappa(\nabla T_h^{n+1}, \nabla S_h) \\ = (g^{n+1}, S_h) \quad \forall S_h \in W_h.$$

Thin wall problem:

$$(28) \quad \left(\frac{u_h^{n+1} - u_h^n}{\Delta t}, v_h \right) + b(< u_h >^n, u_h^{n+1}, v_h) + b(u_h'^n, u_h^n, v_h) + Pr(\nabla u_h^{n+1}, \nabla v_h) - (p_h^{n+1}, \nabla \cdot v_h) \\ = PrRa(\gamma T_h^n, v_h) + (f^{n+1}, v_h) \quad \forall v_h \in X_h,$$

$$(29) \quad (q_h, \nabla \cdot u_h^{n+1}) = 0 \quad \forall q_h \in Q_h,$$

$$(30) \quad \left(\frac{T_h^{n+1} - T_h^n}{\Delta t}, S_h \right) + b^*(< u_h >^n, T_h^{n+1}, S_h) + b^*(u_h'^n, T_h^n, S_h) + \kappa(\nabla T_h^{n+1}, \nabla S_h) \\ = (u_1^n, S_h) + (g^{n+1}, S_h) \quad \forall S_h \in W_h.$$

Remark: The treatment of the nonlinear terms in the time discretizations (5) - (7) and (12) - (14) leads to a shared coefficient matrix independent of the ensemble members.

4. Numerical Analysis of the Ensemble Algorithm. We present stability results for the aforementioned algorithms under the following timestep condition:

$$(31) \quad \frac{C_{\dagger} \Delta t}{h} \max_{1 \leq j \leq J} \|\nabla u_h'^n\|^2 \leq 1,$$

where $C_{\dagger} \equiv C_{\dagger}(|\Omega|, \alpha_{min}, \kappa, Pr)$. In Theorems 4 and 5, the nonlinear stability of the velocity, temperature, and pressure approximations are proven under condition (31) for the thick wall (25) - (27) and thin wall problems (28) - (30), respectively.

Remark: Stability of the numerical approximations can also be proven under: $\frac{JC_{\dagger} \Delta t}{h} < \|\nabla u_h'^n\|^2 \leq 1$. If $C_{\dagger}/J \geq 1$, then JC_{\dagger} can be replaced with C_{\dagger} .

4.1. Stability Analysis.

THEOREM 4. Consider the **Thick wall problem** (25) - (27). Suppose $f \in L^\infty(0, t^*; H^{-1}(\Omega)^d)$, $g \in L^\infty(0, t^*; H^{-1}(\Omega))$. If (25) - (27) satisfy condition (31), then

$$\begin{aligned} & \|T_h^N\|^2 + \|u_h^N\|^2 + \frac{1}{2} \sum_{n=0}^{N-1} (\|T_h^{n+1} - T_h^n\|^2 + \|u_h^{n+1} - u_h^n\|^2) + \kappa \Delta t \|\nabla T_h^N\|^2 + Pr \Delta t \|\nabla u_h^N\|^2 \\ & \leq 2\Delta t Pr Ra^2 C_{PF,1}^2 \sum_{n=0}^{N-1} \left(\frac{\Delta t}{\kappa} \sum_{k=0}^n \|g^{k+1}\|_{-1}^2 + \|T_h^0\|^2 + \kappa \Delta t \|\nabla T_h^0\|^2 \right) + \frac{2\Delta t}{Pr} \sum_{n=0}^{N-1} \|f^{n+1}\|_{-1}^2 + \|u_h^0\|^2 \\ & \quad + Pr \Delta t \|\nabla u_h^0\|^2 + \|T_h^0\|^2 + \kappa \Delta t \|\nabla T_h^0\|^2. \end{aligned}$$

Further,

$$\begin{aligned} \beta \Delta t \sum_{n=0}^{N-1} \|p_h^{n+1}\| & \leq 2\Delta t \sum_{n=0}^{N-1} \left(C_1 \|\nabla \langle u_h \rangle^n\| \|\nabla u_h^{n+1}\| + C_1 \|\nabla u_h'^n\| \|\nabla u_h^n\| \right. \\ & \quad \left. + Pr \|\nabla u_h^{n+1}\| + Pr Ra C_{PF,1} \|T_h^{n+1}\| + \|f^{n+1}\|_{-1} \right). \end{aligned}$$

Proof. Let $S_h = T_h^{n+1}$ in equation (27) and use the polarization identity. Multiply by Δt on both sides and rearrange. Then,

$$(32) \quad \frac{1}{2} \left\{ \|T_h^{n+1}\|^2 - \|T_h^n\|^2 + \|T_h^{n+1} - T_h^n\|^2 \right\} + \kappa \Delta t \|\nabla T_h^{n+1}\|^2 = \Delta t (g^{n+1}, T_h^{n+1}) - \Delta t b^*(u_h'^n, T_h^n, T_h^{n+1}).$$

Use Cauchy-Schwarz-Young on $\Delta t (g^{n+1}, T_h^{n+1})$,

$$(33) \quad \Delta t (g^{n+1}, T_h^{n+1}) \leq \frac{\Delta t}{2\epsilon} \|g^{n+1}\|_{-1}^2 + \frac{\Delta t \epsilon}{2} \|\nabla T_h^{n+1}\|^2.$$

Consider $-\Delta t b^*(u_h'^n, T_h^n, T_h^{n+1})$. Add and subtract $-\Delta t b^*(u_h'^n, T_h^n, T_h^n)$, use skew-symmetry, Lemma 1, the inverse inequality, and the Cauchy-Schwarz-Young inequality. Then,

$$\begin{aligned} (34) \quad |-\Delta t b^*(u_h'^n, T_h^n, T_h^{n+1})| & = |-\Delta t b^*(u_h'^n, T_h^n, T_h^{n+1} - T_h^n)| \\ & \leq \Delta t C_6 \|\nabla u_h'^n\| \|\nabla T_h^n\| \sqrt{\|T_h^{n+1} - T_h^n\| \|\nabla(T_h^{n+1} - T_h^n)\|} \\ & \leq \frac{\Delta t C_6 C_{inv,2}^{1/2}}{h^{1/2}} \|\nabla u_h'^n\| \|\nabla T_h^n\| \|T_h^{n+1} - T_h^n\| \\ & \leq \frac{C_6^2 C_{inv,2} \Delta t^2}{h} \|\nabla u_h'^n\|^2 \|\nabla T_h^n\|^2 + \frac{1}{4} \|T_h^{n+1} - T_h^n\|^2. \end{aligned}$$

Using (33) and (34) in (32) leads to

$$\begin{aligned} & \frac{1}{2} \left\{ \|T_h^{n+1}\|^2 - \|T_h^n\|^2 + \|T_h^{n+1} - T_h^n\|^2 \right\} + \kappa \Delta t \|\nabla T_h^{n+1}\|^2 \leq \frac{\Delta t}{2\epsilon} \|g^{n+1}\|_{-1}^2 \\ & \quad + \frac{\Delta t \epsilon}{2} \|\nabla T_h^{n+1}\|^2 + \frac{C_6^2 C_{inv,2} \Delta t^2}{h} \|\nabla u_h'^n\|^2 \|\nabla T_h^n\|^2 + \frac{1}{4} \|T_h^{n+1} - T_h^n\|^2. \end{aligned}$$

Let $\epsilon = \kappa$, add and subtract $\frac{\kappa \Delta t}{2} \|\nabla T_h^n\|^2$ to the l.h.s. Regrouping terms leads to

$$\begin{aligned} & \frac{1}{2} \left\{ \|T_h^{n+1}\|^2 - \|T_h^n\|^2 \right\} + \frac{1}{4} \|T_h^{n+1} - T_h^n\|^2 + \frac{\kappa \Delta t}{2} \left\{ \|\nabla T_h^{n+1}\|^2 - \|\nabla T_h^n\|^2 \right\} \\ & \quad + \frac{\kappa \Delta t}{2} \|\nabla T_h^n\|^2 \left[1 - \frac{2C_6^2 C_{inv,2} \Delta t}{\kappa h} \|\nabla u_h'^n\|^2 \right] \leq \frac{\Delta t}{2\kappa} \|g^{n+1}\|_{-1}^2. \end{aligned}$$

By hypothesis, $\frac{2C_6^2 C_{inv,2} \Delta t}{\kappa h} \|\nabla u_h'^n\|^2 \leq 1$. Thus,

$$\frac{1}{2} \left\{ \|T_h^{n+1}\|^2 - \|T_h^n\|^2 \right\} + \frac{1}{4} \|T_h^{n+1} - T_h^n\|^2 + \frac{\kappa \Delta t}{2} \left\{ \|\nabla T_h^{n+1}\|^2 - \|\nabla T_h^n\|^2 \right\} \leq \frac{\Delta t}{2\kappa} \|g^{n+1}\|_{-1}^2.$$

Sum from $n = 0$ to $n = N - 1$ and put all data on the right hand side. This yields

$$(35) \quad \frac{1}{2} \|T_h^N\|^2 + \frac{1}{4} \sum_{n=0}^{N-1} \|T_h^{n+1} - T_h^n\|^2 + \frac{\kappa \Delta t}{2} \|\nabla T_h^N\|^2 \leq \frac{\Delta t}{2\kappa} \sum_{n=0}^{N-1} \|g^{n+1}\|_{-1}^2 + \frac{1}{2} \|T_h^0\|^2 + \frac{\kappa \Delta t}{2} \|\nabla T_h^0\|^2.$$

Therefore, the l.h.s. is bounded by data on the r.h.s. The temperature approximation is stable.

We follow an almost identical form of attack for the velocity as we did for the temperature. Let $v_h = u_h^{n+1} \in V_h$ in (25) and use the polarization identity. Multiply by Δt on both sides and rearrange terms. Then,

$$(36) \quad \frac{1}{2} \left\{ \|u_h^{n+1}\|^2 - \|u_h^n\|^2 + \|u_h^{n+1} - u_h^n\|^2 \right\} + \Delta t Pr \|\nabla u_h^{n+1}\|^2 \\ = -\Delta t b(u_h'^n, u_h^n, u_h^{n+1}) + \Delta t Pr Ra(\gamma T_h^{n+1}, u_h^{n+1}) + \Delta t (f^{n+1}, u_h^{n+1}).$$

Use the Cauchy-Schwarz-Young inequality on $\Delta t Pr Ra(\gamma T_h^{n+1}, u_h^{n+1})$ and $\Delta t (f^{n+1}, u_h^{n+1})$ and note that $|\gamma| = 1$,

$$(37) \quad \Delta t Pr Ra(\gamma T_h^{n+1}, u_h^{n+1}) \leq \frac{\Delta t Pr^2 Ra^2 C_{PF,1}^2}{2\epsilon} \|T_h^{n+1}\|^2 + \frac{\Delta t \epsilon}{2} \|\nabla u_h^{n+1}\|^2,$$

$$(38) \quad \Delta t (f^{n+1}, u_h^{n+1}) \leq \frac{\Delta t}{2\epsilon} \|f^{n+1}\|_{-1}^2 + \frac{\Delta t \epsilon}{2} \|\nabla u_h^{n+1}\|^2.$$

Using skew-symmetry, Lemma 1, the inverse inequality, and the Cauchy-Schwarz-Young inequality on $\Delta t b(u_h'^n, u_h^n, u_h^{n+1})$ leads to

$$(39) \quad |-\Delta t b(u_h'^n, u_h^n, u_h^{n+1})| \leq \frac{C_5^2 C_{inv,1} \Delta t^2}{h} \|\nabla u_h'^n\|^2 \|\nabla u_h^n\|^2 + \frac{1}{4} \|u_h^{n+1} - u_h^n\|^2.$$

Using (37), (38), and (39) in (36) leads to

$$\frac{1}{2} \left\{ \|u_h^{n+1}\|^2 - \|u_h^n\|^2 + \|u_h^{n+1} - u_h^n\|^2 \right\} + Pr \Delta t \|\nabla u_h^{n+1}\|^2 \leq \frac{\Delta t Pr^2 Ra^2 C_{PF,1}^2}{2\epsilon} \|T_h^{n+1}\|^2 + \frac{\Delta t}{2\epsilon} \|f^{n+1}\|_{-1}^2 \\ + \Delta t \epsilon \|\nabla u_h^{n+1}\|^2 + \frac{C_5^2 C_{inv,1} \Delta t^2}{h} \|\nabla u_h'^n\|^2 \|\nabla u_h^n\|^2 + \frac{1}{4} \|u_h^{n+1} - u_h^n\|^2.$$

Let $\epsilon = Pr/2$, add and subtract $\frac{Pr \Delta t}{2} \|\nabla u_h^n\|^2$ to the l.h.s., and regroup terms. Then,

$$\frac{1}{2} \left\{ \|u_h^{n+1}\|^2 - \|u_h^n\|^2 \right\} + \frac{1}{4} \|u_h^{n+1} - u_h^n\|^2 + \frac{Pr \Delta t}{2} \left\{ \|\nabla u_h^{n+1}\|^2 - \|\nabla u_h^n\|^2 \right\} \\ + \frac{Pr \Delta t}{2} \|\nabla u_h^n\|^2 \left[1 - \frac{2C_5^2 C_{inv,1} \Delta t}{Pr h} \|\nabla u_h'^n\|^2 \right] \leq \Delta t Pr Ra^2 C_{PF,1}^2 \|T_h^{n+1}\|^2 + \frac{\Delta t}{Pr} \|f^{n+1}\|_{-1}^2.$$

By hypothesis, $\frac{2C_5^2 C_{inv,1} \Delta t}{Pr h} \|\nabla u_h'^n\|^2 \leq 1$. Thus,

$$\frac{1}{2} \left\{ \|u_h^{n+1}\|^2 - \|u_h^n\|^2 \right\} + \frac{1}{4} \|u_h^{n+1} - u_h^n\|^2 + \frac{Pr \Delta t}{2} \left\{ \|\nabla u_h^{n+1}\|^2 - \|\nabla u_h^n\|^2 \right\} \\ \leq \Delta t Pr Ra^2 C_{PF,1}^2 \|T_h^{n+1}\|^2 + \frac{\Delta t}{Pr} \|f^{n+1}\|_{-1}^2.$$

Summing from $n = 0$ to $n = N - 1$ and putting all data on r.h.s. yields

$$(40) \quad \frac{1}{2} \|u_h^N\|^2 + \frac{1}{4} \sum_{n=0}^{N-1} \|u_h^{n+1} - u_h^n\|^2 + \frac{Pr \Delta t}{2} \|\nabla u_h^N\|^2 \leq \Delta t Pr Ra^2 C_{PF,1}^2 \sum_{n=0}^{N-1} \|T_h^{n+1}\|^2 + \frac{\Delta t}{Pr} \sum_{n=0}^{N-1} \|f^{n+1}\|_{-1}^2 \\ + \frac{1}{2} \|u_h^0\|^2 + \frac{Pr \Delta t}{2} \|\nabla u_h^0\|^2.$$

Together with the stability of the temperature approximation, the l.h.s. is bounded above by data; that is, the velocity approximation is stable. Adding (35) and (40) and multiplying by 2 yields the result. We now prove stability of the pressure approximation. We first form an estimate for the discrete time derivative term. Consider (25), isolate $(\frac{u_h^{n+1}-u_h^n}{\Delta t}, v_h)$, let $0 \neq v_h \in V_h$, and multiply by Δt . Then,

$$(41) \quad (u_h^{n+1} - u_h^n, v_h) = -\Delta t b(\langle u_h \rangle^n, u_h^{n+1}, v_h) - \Delta t b(u_h'^n, u_h^n, v_h) \\ - \Delta t Pr(\nabla u_h^{n+1}, \nabla v_h) + \Delta t Pr Ra(\gamma T_h^{n+1}, v_h) + \Delta t(f^{n+1}, v_h).$$

Applying Lemma 1 to the skew-symmetric trilinear terms and the Cauchy-Schwarz and Poincaré-Friedrichs inequalities to the remaining terms yields

$$(42) \quad |-\Delta t b(\langle u_h \rangle^n, u_h^{n+1}, v_h)| \leq C_1 \Delta t \|\nabla \langle u_h \rangle^n\| \|\nabla u_h^{n+1}\| \|\nabla v_h\|,$$

$$(43) \quad |-\Delta t b(u_h'^n, u_h^n, v_h)| \leq C_1 \Delta t \|\nabla u_h'^n\| \|\nabla u_h^n\| \|\nabla v_h\|,$$

$$(44) \quad |-\Delta t Pr(\nabla u_h^{n+1}, \nabla v_h)| \leq Pr \Delta t \|\nabla u_h^{n+1}\| \|\nabla v_h\|,$$

$$(45) \quad |\Delta t Pr Ra(\gamma T_h^{n+1}, v_h)| \leq Pr Ra \Delta t \|T_h^{n+1}\| \|v_h\| \leq Pr Ra C_{PF,1} \Delta t \|T_h^{n+1}\| \|\nabla v_h\|,$$

$$(46) \quad |\Delta t(f^{n+1}, v_h)| \leq \Delta t \|f^{n+1}\|_{-1} \|\nabla v_h\|.$$

Apply the above estimates in (41), divide by the common factor $\|\nabla v_h\|$ on both sides, and take the supremum over all $0 \neq v_h \in V_h$. Then,

$$(47) \quad \|u_h^{n+1} - u_h^n\|_{V_h^*} \leq C_1 \Delta t \|\nabla \langle u_h \rangle^n\| \|\nabla u_h^{n+1}\| + C_1 \Delta t \|\nabla u_h'^n\| \|\nabla u_h^n\| \\ + Pr \Delta t \|\nabla u_h^{n+1}\| + Pr Ra C_{PF,1} \Delta t \|T_h^{n+1}\| + \Delta t \|f^{n+1}\|_{-1}.$$

Reconsider equation (25). Multiply by Δt and isolate the pressure term,

$$(48) \quad \Delta t(p_h^{n+1}, \nabla \cdot v_h) = (u_h^{n+1} - u_h^n, v_h) + \Delta t b(\langle u_h \rangle^n, u_h^{n+1}, v_h) + \Delta t b(u_h'^n, u_h^n, v_h) \\ + Pr \Delta t(\nabla u_h^{n+1}, \nabla v_h) - Pr Ra \Delta t(\gamma T_h^{n+1}, v_h) - \Delta t(f^{n+1}, v_h).$$

Apply (42) - (46) on the r.h.s terms. Then,

$$(49) \quad \Delta t(p_h^{n+1}, \nabla \cdot v_h) \leq (u_h^{n+1} - u_h^n, v_h) + \left(C_1 \Delta t \|\nabla \langle u_h \rangle^n\| \|\nabla u_h^{n+1}\| + C_1 \Delta t \|\nabla u_h'^n\| \|\nabla u_h^n\| \right. \\ \left. + Pr \Delta t \|\nabla u_h^{n+1}\| + Pr Ra C_{PF,1} \Delta t \|T_h^{n+1}\| + \Delta t \|f^{n+1}\|_{-1} \right) \|\nabla v_h\|.$$

Divide by $\|\nabla v_h\|$ and note that $\frac{(u_h^{n+1}-u_h^n, v_h)}{\|\nabla v_h\|} \leq \|u_h^{n+1} - u_h^n\|_{V_h^*}$. Take the supremum over all $0 \neq v_h \in X_h$,

$$(50) \quad \Delta t \sup_{0 \neq v_h \in X_h} \frac{(p_h^{n+1}, \nabla \cdot v_h)}{\|\nabla v_h\|} \leq 2 \left(C_1 \Delta t \|\nabla \langle u_h \rangle^n\| \|\nabla u_h^{n+1}\| + C_1 \Delta t \|\nabla u_h'^n\| \|\nabla u_h^n\| \right. \\ \left. + Pr \Delta t \|\nabla u_h^{n+1}\| + Pr Ra C_{PF,1} \Delta t \|T_h^{n+1}\| + \Delta t \|f^{n+1}\|_{-1} \right).$$

Use the discrete inf-sup condition (24),

$$(51) \quad \beta \Delta t \|p_h^{n+1}\| \leq 2 \left(C_1 \Delta t \|\nabla \langle u_h \rangle^n\| \|\nabla u_h^{n+1}\| + C_1 \Delta t \|\nabla u_h'^n\| \|\nabla u_h^n\| \right. \\ \left. + Pr \Delta t \|\nabla u_h^{n+1}\| + Pr Ra C_{PF,1} \Delta t \|T_h^{n+1}\| + \Delta t \|f^{n+1}\|_{-1} \right).$$

Summing from $n = 0$ to $n = N - 1$ yields stability of the pressure approximation, built on the stability of the temperature and velocity approximations. \square

THEOREM 5. Consider the **Thin wall problem** (28) - (30). Suppose $f \in L^\infty(0, t^*; H^{-1}(\Omega)^d)$ and $g \in L^\infty(0, t^*; H^{-1}(\Omega))$. If (28) - (30) satisfy condition (31), then

$$\begin{aligned} \|T_h^N\|^2 + \|u_h^N\|^2 + \frac{1}{2} \sum_{n=0}^{N-1} (\|T_h^{n+1} - T_h^n\|^2 + \|u_h^{n+1} - u_h^n\|^2) + \kappa \Delta t \|\nabla T_h^N\|^2 + Pr \Delta t \|\nabla u_h^N\|^2 \\ \leq \exp(2Ct^*) \left\{ \Delta t \sum_{n=0}^{N-1} \left(\frac{1}{Pr} \|f^{n+1}\|_{-1}^2 + \frac{1}{\kappa} \|g^{n+1}\|_{-1}^2 \right) + \|u_h^0\|^2 + \|T_h^0\|^2 \right. \\ \left. + Pr \Delta t \|\nabla u_h^0\|^2 + \kappa \Delta t \|\nabla T_h^0\|^2 \right\}. \end{aligned}$$

Further,

$$\begin{aligned} \beta \Delta t \sum_{n=0}^{N-1} \|p_h^{n+1}\| \leq 2 \sum_{n=0}^{N-1} \left(C_1 \Delta t \|\nabla \langle u_h \rangle^n\| \|\nabla u_h^{n+1}\| + C_1 \Delta t \|\nabla u_h'^n\| \|\nabla u_h^n\| \right. \\ \left. + Pr \Delta t \|\nabla u_h^{n+1}\| + Pr Ra C_{PF,1} \Delta t \|T_h^n\| + \Delta t \|f^{n+1}\|_{-1} \right). \end{aligned}$$

Proof. Add equations (28) and (30), let $S_h = T_h^{n+1} \in W_h$ and $v_h = u_h^{n+1} \in V_h$ and use the polarization identity. Then,

$$\begin{aligned} (52) \quad \frac{1}{2\Delta t} \left\{ \|T_h^{n+1}\|^2 - \|T_h^n\|^2 + \|T_h^{n+1} - T_h^n\|^2 \right\} + \frac{1}{2\Delta t} \left\{ \|u_h^{n+1}\|^2 - \|u_h^n\|^2 + \|u_h^{n+1} - u_h^n\|^2 \right\} \\ + \kappa \|\nabla T_h^{n+1}\|^2 + Pr \|\nabla u_h^{n+1}\|^2 + b(u_h^n, u_h^n, u_h^{n+1}) + b^*(u_h^n, T_h^n, T_h^{n+1}) = Pr Ra (\gamma T_h^n, u_h^{n+1}) \\ + (u_h^n, T_h^{n+1}) + (f^{n+1}, u_h^{n+1}) + (g^{n+1}, T_h^{n+1}). \end{aligned}$$

Apply similar techniques and estimates as in the proof of Theorem 4,

$$\begin{aligned} (53) \quad \frac{1}{2} \left\{ \|T_h^{n+1}\|^2 - \|T_h^n\|^2 + \|T_h^{n+1} - T_h^n\|^2 \right\} + \frac{1}{2} \left\{ \|u_h^{n+1}\|^2 - \|u_h^n\|^2 + \|u_h^{n+1} - u_h^n\|^2 \right\} \\ + \frac{\kappa \Delta t}{2} \left\{ \|\nabla T_h^{n+1}\|^2 - \|\nabla T_h^n\|^2 \right\} + \frac{Pr \Delta t}{2} \left\{ \|\nabla u_h^{n+1}\|^2 - \|\nabla u_h^n\|^2 \right\} \\ + \frac{\kappa \Delta t}{2} \|\nabla T_h^n\|^2 \left\{ 1 - \frac{2\Delta t C_6^2 C_{inv,2}}{\kappa h} \|\nabla u_h'^n\|^2 \right\} + \frac{Pr \Delta t}{2} \|\nabla u_h^n\|^2 \left\{ 1 - \frac{2\Delta t C_5^2 C_{inv,1}}{Pr h} \|\nabla u_h'^n\|^2 \right\} \\ \leq \Delta t Pr Ra^2 C_{PF,1}^2 \|T_h^n\|^2 + \frac{\Delta t C_{PF,2}^2}{\kappa} \|u_h^n\|^2 + \frac{\Delta t}{Pr} \|f^{n+1}\|_{-1}^2 + \frac{\Delta t}{\kappa} \|g^{n+1}\|_{-1}^2. \end{aligned}$$

Using the timestep condition, multiplying by 2, taking a maximum over constants in the first two terms on the r.h.s. and summing from $n = 0$ to $n = N - 1$ leads to,

$$\begin{aligned} (54) \quad \|T_h^N\|^2 + \|u_h^N\|^2 + \frac{1}{2} \sum_{n=0}^{N-1} (\|T_h^{n+1} - T_h^n\|^2 + \|u_h^{n+1} - u_h^n\|^2) + \kappa \Delta t \|\nabla T_h^N\|^2 + Pr \Delta t \|\nabla u_h^N\|^2 \\ \leq C \Delta t \sum_{n=0}^{N-1} \left\{ \|T_h^n\|^2 + \|u_h^n\|^2 \right\} + 2\Delta t \sum_{n=0}^{N-1} \left\{ \frac{1}{Pr} \|f^{n+1}\|_{-1}^2 + \frac{1}{\kappa} \|g^{n+1}\|_{-1}^2 \right\} + \|u_h^0\|^2 + \|T_h^0\|^2 \\ + Pr \Delta t \|\nabla u_h^0\|^2 + \kappa \Delta t \|\nabla T_h^0\|^2. \end{aligned}$$

Lastly, apply Lemma 3. Then,

$$\begin{aligned} (55) \quad \|T_h^N\|^2 + \|u_h^N\|^2 + \frac{1}{2} \sum_{n=0}^{N-1} (\|T_h^{n+1} - T_h^n\|^2 + \|u_h^{n+1} - u_h^n\|^2) + \kappa \Delta t \|\nabla T_h^N\|^2 + Pr \Delta t \|\nabla u_h^N\|^2 \\ \leq \exp(Ct^*) \left\{ 2\Delta t \sum_{n=0}^{N-1} \left(\frac{1}{Pr} \|f^{n+1}\|_{-1}^2 + \frac{1}{\kappa} \|g^{n+1}\|_{-1}^2 \right) + \|u_h^0\|^2 + \|T_h^0\|^2 \right. \\ \left. + Pr \Delta t \|\nabla u_h^0\|^2 + \kappa \Delta t \|\nabla T_h^0\|^2 \right\}. \end{aligned}$$

Thus, numerical approximations of velocity and temperature are stable. Stability of the pressure approximation follows by similar arguments as in Theorem 4. \square

Remark: Theorem 4 implies long-time stability of the approximate solutions. Application of Lemma 3 in Theorem 5 leads to the loss of long-time stability due to the exponential growth factor, in t^* .

4.2. Error Analysis. Denote u^n , p^n , and T^n as the true solutions at time $t^n = n\Delta t$. Assume the solutions satisfy the following regularity assumptions:

$$(56) \quad \begin{aligned} u &\in L^\infty(0, t^*; X \cap H^{k+1}(\Omega)), \quad T \in L^\infty(0, t^*; W \cap H^{k+1}(\Omega)), \\ u_t, T_t &\in L^\infty(0, t^*; H^{k+1}(\Omega)), \quad u_{tt}, T_{tt} \in L^\infty(0, t^*; L^2(\Omega)), \\ p &\in L^\infty(0, t^*; Q \cap H^m(\Omega)). \end{aligned}$$

The errors are denoted

$$e_u^n = u^n - u_h^n, \quad e_T^n = T^n - T_h^n, \quad e_p^n = p^n - p_h^n.$$

DEFINITION 6. (Consistency error). The consistency errors are defined as

$$\tau_u(u^n; v_h) = \left(\frac{u^n - u^{n-1}}{\Delta t} - u_t^n, v_h \right), \quad \tau_T(T^n; S_h) = \left(\frac{T^n - T^{n-1}}{\Delta t} - T_t^n, S_h \right).$$

LEMMA 7. Provided u and T satisfy the regularity assumptions (56), then $\forall r > 0$

$$\begin{aligned} |\tau_u(u^n; v_h)| &\leq \frac{C_{PF,1}^2 C_r \Delta t^2}{\epsilon} \|u_{tt}\|_{L^\infty(t^{n-1}, t^n; L^2(\Omega))}^2 + \frac{\epsilon}{r} \|\nabla v_h\|^2, \\ |\tau_T(T^n; S_h)| &\leq \frac{C_{PF,2}^2 C_r \Delta t^2}{\epsilon} \|T_{tt}\|_{L^\infty(t^{n-1}, t^n; L^2(\Omega))}^2 + \frac{\epsilon}{r} \|\nabla S_h\|^2. \end{aligned}$$

Proof. These follow from the Cauchy-Schwarz-Young inequality, Poincaré-Friedrichs inequality, and Taylor's Theorem with integral remainder. \square

THEOREM 8. For (u, p, T) satisfying (1) - (5), suppose that $(u_h^0, p_h^0, T_h^0) \in (X_h, Q_h, W_h)$ are approximations of (u^0, p^0, T^0) to within the accuracy of the interpolant. Further, suppose that condition (31) holds. Then there exists a constant C such that

$$\begin{aligned} &\|e_T^N\|^2 + \|e_u^N\|^2 + \frac{1}{2} \sum_{n=0}^{N-1} (\|e_T^{n+1} - e_T^n\|^2 + \|e_u^{n+1} - e_u^n\|^2) + \frac{\kappa \Delta t}{2} \|\nabla e_T^N\|^2 + \frac{Pr \Delta t}{2} \|\nabla e_u^N\|^2 \\ &\leq C \left\{ \Delta t \inf_{v_h \in X_h} \left(\|\nabla(u - v_h)\|_{\infty,0}^2 + \|(u - v_h)_t\|_{\infty,0}^2 \right) + \Delta t \inf_{S_h \in W_h} \left(\|\nabla(T - S_h)\|_{\infty,0}^2 + \|(T - S_h)_t\|_{\infty,0}^2 \right) \right. \\ &\quad + \Delta t \inf_{q_h \in Q_h} \|p - q_h\|_{\infty,0}^2 + \Delta t^3 + \Delta t \|\nabla \eta^0\|^2 + \Delta t \|\nabla \zeta^0\|^2 + \|\eta^0\|^2 \\ &\quad \left. + \|\zeta^0\|^2 + \|e_T^0\|^2 + \|e_u^0\|^2 + \Delta t \|\nabla e_T^0\|^2 + \Delta t \|\nabla e_u^0\|^2 \right\}. \end{aligned}$$

Proof. The true solutions satisfy for all $n = 0, 1, \dots, N$:

$$(57) \quad \left(\frac{u^{n+1} - u^n}{\Delta t}, v_h \right) + b(u^{n+1}, u^{n+1}, v_h) + Pr(\nabla u^{n+1}, \nabla v_h) - (p^{n+1}, \nabla \cdot v_h) = PrRa(\gamma T^{n+1}, v_h)$$

$$(58) \quad \begin{aligned} &+ (f^{n+1}, v_h) + \tau_u(u^{n+1}, v_h) \quad \forall v_h \in X_h, \\ &(q_h, \nabla \cdot u^{n+1}) = 0 \quad \forall q_h \in Q_h, \end{aligned}$$

$$(59) \quad \left(\frac{T^{n+1} - T^n}{\Delta t}, S_h \right) + b^*(u^{n+1}, T^{n+1}, S_h) + \kappa(\nabla T^{n+1}, \nabla S_h) = (g^{n+1}, S_h) + \tau_T(T^{n+1}, S_h) \quad \forall S_h \in W_h.$$

Subtract (59) and (27), then the error equation for temperature is

$$(60) \quad \left(\frac{e_T^{n+1} - e_T^n}{\Delta t}, S_h \right) + b^*(u^{n+1}, T^{n+1}, S_h) - b^*(u_h^n - u_h'^n, T_h^{n+1}, S_h) - b^*(u_h'^n, T_h^n, S_h) \\ + \kappa(\nabla e_T^{n+1}, \nabla S_h) = \tau_T(T^{n+1}, S_h) \quad \forall S_h \in W_h.$$

Letting $e_T^n = (T^n - \tilde{T}^n) - (T_h^n - \tilde{T}_h^n) = \zeta^n - \psi_h^n$ and rearranging give,

$$\left(\frac{\psi_h^{n+1} - \psi_h^n}{\Delta t}, S_h \right) + \kappa(\nabla \psi_h^{n+1}, \nabla S_h) = \left(\frac{\zeta^{n+1} - \zeta^n}{\Delta t}, S_h \right) + \kappa(\nabla \zeta^{n+1}, \nabla S_h) - \tau_T(T^{n+1}, S_h) \\ + b^*(u^{n+1}, T^{n+1}, S_h) - b^*(u_h^n - u_h'^n, T_h^{n+1}, S_h) - b^*(u_h'^n, T_h^n, S_h) \quad \forall S_h \in W_h.$$

Set $S_h = \psi_h^{n+1} \in W_h$. This yields

$$(61) \quad \frac{1}{2\Delta t} \left\{ \|\psi_h^{n+1}\|^2 - \|\psi_h^n\|^2 + \|\psi_h^{n+1} - \psi_h^n\|^2 \right\} + \kappa \|\nabla \psi_h^{n+1}\|^2 = \frac{1}{\Delta t} (\zeta^{n+1} - \zeta^n, \psi_h^{n+1}) + \kappa(\nabla \zeta^{n+1}, \nabla \psi_h^{n+1}) \\ - \tau_T(T^{n+1}, \psi_h^{n+1}) + b^*(u^{n+1}, T^{n+1}, \psi_h^{n+1}) - b^*(u_h^n - u_h'^n, T_h^{n+1}, \psi_h^{n+1}) - b^*(u_h'^n, T_h^n, \psi_h^{n+1}).$$

Add and subtract $b^*(u^{n+1}, T_h^{n+1}, \psi_h^{n+1})$, $b^*(u^n, T_h^{n+1}, \psi_h^{n+1})$, and $b^*(u_h'^n, T^{n+1} - T^n, \psi_h^{n+1})$. Then,

$$(62) \quad \frac{1}{2\Delta t} \left\{ \|\psi_h^{n+1}\|^2 - \|\psi_h^n\|^2 + \|\psi_h^{n+1} - \psi_h^n\|^2 \right\} + \kappa \|\nabla \psi_h^{n+1}\|^2 = \frac{1}{\Delta t} (\zeta^{n+1} - \zeta^n, \psi_h^{n+1}) + \kappa(\nabla \zeta^{n+1}, \nabla \psi_h^{n+1}) \\ + b^*(u^{n+1}, \zeta^{n+1}, \psi_h^{n+1}) + b^*(u^{n+1} - u^n, T_h^{n+1}, \psi_h^{n+1}) + b^*(\eta^n, T_h^{n+1}, \psi_h^{n+1}) \\ - b^*(\phi_h^n, T_h^{n+1}, \psi_h^{n+1}) + b^*(u_h'^n, \zeta^{n+1}, \psi_h^{n+1}) - b^*(u_h'^n, \zeta^n, \psi_h^{n+1}) + b^*(u_h'^n, \psi_h^n, \psi_h^{n+1}) \\ + b^*(u_h'^n, T^{n+1} - T^n, \psi_h^{n+1}) - \tau_T(T^{n+1}, \psi_h^{n+1}).$$

Follow analogously for the velocity error equation. Subtract (57) and (25), split the error into $e_u^n = (u^n - \tilde{u}^n) - (u_h^n - \tilde{u}_h^n) = \eta^n - \phi_h^n$, let $v_h = \phi_h^{n+1} \in V_h$, add and subtract $b(u^{n+1}, u_h^{n+1}, \phi_h^{n+1})$, $b(u^n, u_h^{n+1}, \phi_h^{n+1})$, and $b(u_h'^n, u^{n+1} - u^n, \phi_h^{n+1})$. Then,

$$(63) \quad \frac{1}{2\Delta t} \left\{ \|\phi_h^{n+1}\|^2 - \|\phi_h^n\|^2 + \|\phi_h^{n+1} - \phi_h^n\|^2 \right\} + Pr \|\nabla \phi_h^{n+1}\|^2 = \frac{1}{\Delta t} (\eta^{n+1} - \eta^n, \phi_h^{n+1}) \\ + Pr(\nabla \eta^{n+1}, \nabla \phi_h^{n+1}) - (p^{n+1} - q_h^{n+1}, \nabla \cdot \phi_h^{n+1}) + PrRa(\gamma \zeta^{n+1}, \phi_h^{n+1}) \\ - PrRa(\gamma \psi_h^{n+1}, \phi_h^{n+1}) + b(u^{n+1}, \eta^{n+1}, \phi_h^{n+1}) + b(u^{n+1} - u^n, u_h^{n+1}, \phi_h^{n+1}) + b(\eta^n, u_h^{n+1}, \phi_h^{n+1}) \\ - b(\phi_h^n, u_h^{n+1}, \phi_h^{n+1}) + b(u_h'^n, \eta^{n+1}, \phi_h^{n+1}) - b(u_h'^n, \eta^n, \phi_h^{n+1}) + b(u_h'^n, \phi_h^n, \phi_h^{n+1}) \\ + b(u_h'^n, u^{n+1} - u^n, \phi_h^{n+1}) - \tau_u(u^{n+1}, \phi_h^{n+1}).$$

Our goal now is to estimate all terms on the r.h.s. in such a way that we may hide the terms involving unknown pieces ψ_h^k into the l.h.s. The following estimates are formed using Lemma 1 in conjunction with the Cauchy-Schwarz-Young inequality,

$$(64) \quad |b^*(u^{n+1}, \zeta^{n+1}, \psi_h^{n+1})| \leq C_3 \|\nabla u^{n+1}\| \|\nabla \zeta^{n+1}\| \|\nabla \psi_h^{n+1}\| \leq \frac{C_r C_3^2}{\epsilon_3} \|\nabla u^{n+1}\|^2 \|\nabla \zeta^{n+1}\|^2 + \frac{\epsilon_3}{r} \|\nabla \psi_h^{n+1}\|^2,$$

$$(65) \quad |b^*(\eta^n, T_h^{n+1}, \psi_h^{n+1})| \leq C_3 \|\nabla \eta^n\| \|\nabla T_h^{n+1}\| \|\nabla \psi_h^{n+1}\| \leq \frac{C_r C_3^2}{\epsilon_5} \|\nabla \eta^n\|^2 \|\nabla T_h^{n+1}\|^2 + \frac{\epsilon_5}{r} \|\nabla \psi_h^{n+1}\|^2,$$

$$(66) \quad |b^*(u_h'^n, \zeta^{n+1}, \psi_h^{n+1})| \leq C_3 \|u_h'^n\| \|\zeta^{n+1}\| \|\psi_h^{n+1}\| \leq \frac{C_r C_3^2}{\epsilon_7} \|\nabla u_h'^n\|^2 \|\nabla \zeta^{n+1}\|^2 + \frac{\epsilon_7}{r} \|\nabla \psi_h^{n+1}\|^2,$$

$$(67) \quad |-b^*(u_h'^n, \zeta^n, \psi_h^{n+1})| \leq C_3 \|\nabla u_h'^n\| \|\nabla \zeta^n\| \|\nabla \psi_h^{n+1}\| \leq \frac{C_r C_3^2}{\epsilon_8} \|\nabla u_h'^n\|^2 \|\nabla \zeta^n\|^2 + \frac{\epsilon_8}{r} \|\nabla \psi_h^{n+1}\|^2.$$

Applying Lemma 1, the Cauchy-Schwarz-Young inequality, and Taylor's theorem yields,

$$\begin{aligned}
(68) \quad |b^*(u^{n+1} - u^n, T_h^{n+1}, \psi_h^{n+1})| &\leq C_3 \|\nabla(u^{n+1} - u^n)\| \|\nabla T_h^{n+1}\| \|\nabla \psi_h^{n+1}\| \\
&\leq \frac{C_r C_3^2}{\epsilon_4} \|\nabla(u^{n+1} - u^n)\|^2 \|\nabla T_h^{n+1}\|^2 + \frac{\epsilon_4}{r} \|\nabla \psi_h^{n+1}\|^2 \\
&\leq \frac{C_r C_3^2 \Delta t^2}{\epsilon_4} \|\nabla T_h^{n+1}\|^2 \|\nabla u_t\|_{L^\infty(t^n, t^{n+1}; L^2(\Omega))}^2 + \frac{\epsilon_4}{r} \|\nabla \psi_h^{n+1}\|^2, \\
(69) \quad |b^*(u_h^n, T^{n+1} - T^n, \psi_h^{n+1})| &\leq C_3 \|\nabla u_h^n\| \|\nabla(T^{n+1} - T^n)\| \|\nabla \psi_h^{n+1}\| \\
&\leq \frac{C_r C_3^2 \Delta t^2}{\epsilon_{10}} \|\nabla u_h^n\|^2 \|\nabla T_t\|_{L^\infty(t^n, t^{n+1}; L^2(\Omega))}^2 + \frac{\epsilon_{10}}{r} \|\nabla \psi_h^{n+1}\|^2.
\end{aligned}$$

Apply Lemma 1 and the Cauchy-Schwarz-Young inequality twice. This yields

$$\begin{aligned}
(70) \quad |-b^*(\phi_h^n, T_h^{n+1}, \psi_h^{n+1})| &\leq C_4 \sqrt{\|\phi_h^n\| \|\nabla \phi_h^n\|} \|\nabla T_h^{n+1}\| \|\nabla \psi_h^{n+1}\| \leq C_4 C_T(j) \sqrt{\|\phi_h^n\| \|\nabla \phi_h^n\|} \|\nabla \psi_h^{n+1}\| \\
&\leq \frac{C_4 C_T \epsilon_6}{2} \|\nabla \psi_h^{n+1}\|^2 + \frac{C_4 C_T \delta_6}{4 \epsilon_6} \|\nabla \phi_h^n\|^2 + \frac{C_4 C_T}{4 \epsilon_6 \delta_6} \|\phi_h^n\|^2.
\end{aligned}$$

Use Lemma 1, the inverse inequality, and the Cauchy-Schwarz-Young inequality yielding

$$\begin{aligned}
(71) \quad |\Delta t b^*(u_h^n, \psi_h^n, \psi_h^{n+1})| &= |\Delta t b^*(u_h^n, \psi_h^n, \psi_h^{n+1} - \psi_h^n)| \\
&\leq \Delta t C_6 \|\nabla u_h^n\| \|\nabla \psi_h^n\| \sqrt{\|\psi_h^{n+1} - \psi_h^n\| \|\nabla(\psi_h^{n+1} - \psi_h^n)\|} \\
&\leq \frac{\Delta t C_6 C_{inv,2}^{1/2}}{h^{1/2}} \|\nabla u_h^n\| \|\nabla \psi_h^n\| \|\psi_h^{n+1} - \psi_h^n\| \\
&\leq \frac{C_6^2 C_{inv,2} \Delta t}{2 h \epsilon_9} \|\nabla u_h^n\|^2 \|\nabla \psi_h^n\|^2 + \frac{\epsilon_9}{2} \|\psi_h^{n+1} - \psi_h^n\|^2.
\end{aligned}$$

The Cauchy-Schwarz-Young inequality, Poincaré-Friedrichs inequality and Taylor's theorem yield

$$(72) \quad \left| \frac{1}{\Delta t} (\zeta^{n+1} - \zeta^n, \psi_h^{n+1}) \right| \leq \frac{C_{PF,2}^2 C_r}{\epsilon_1} \|\zeta_t\|_{L^\infty(t^n, t^{n+1}; L^2(\Omega))}^2 + \frac{\epsilon_1}{r} \|\nabla \psi_h^{n+1}\|^2.$$

Lastly, use the Cauchy-Schwarz-Young inequality,

$$(73) \quad |\kappa(\nabla \zeta^{n+1}, \nabla \psi_h^{n+1})| \leq \frac{C_r \kappa^2}{\epsilon_2} \|\nabla \zeta^{n+1}\|^2 + \frac{\epsilon_2}{r} \|\nabla \psi_h^{n+1}\|^2.$$

Similar estimates follow for the r.h.s. terms in (63), however, we must treat an additional pressure term and error term,

$$(74) \quad |-(p^{n+1} - q_h^{n+1}, \nabla \cdot \phi_h^{n+1})| \leq \sqrt{d} \|p^{n+1} - q_h^{n+1}\| \|\nabla \phi_h^{n+1}\| \leq \frac{d C_r}{\epsilon_{14}} \|p^{n+1} - q_h^{n+1}\|^2 + \frac{\epsilon_{14}}{r} \|\nabla \phi_h^{n+1}\|^2,$$

$$(75) \quad |Pr Ra(\gamma \zeta^{n+1}, \phi_h^{n+1})| \leq \frac{Pr^2 Ra^2 C_{PF,1}^2 C_{PF,2}^2 C_r}{\epsilon_{15}} \|\nabla \zeta^{n+1}\|^2 + \frac{\epsilon_{15}}{r} \|\nabla \phi_h^{n+1}\|^2,$$

$$(76) \quad | -Pr Ra(\gamma \psi_h^{n+1}, \phi_h^{n+1}) | \leq \frac{Pr^2 Ra^2 C_{PF,1}^2 C_{PF,2}^2 C_r}{\epsilon_{16}} \|\nabla \psi_h^{n+1}\|^2 + \frac{\epsilon_{16}}{r} \|\nabla \phi_h^{n+1}\|^2.$$

Applying the estimates and Lemma 7 into the temperature and velocity error equations (62), (63) and

multiplying by Δt :

$$\begin{aligned}
(77) \quad & \frac{1}{2} \left\{ \|\psi_h^{n+1}\|^2 - \|\psi_h^n\|^2 + \|\psi_h^{n+1} - \psi_h^n\|^2 \right\} + \kappa \Delta t \|\nabla \psi_h^{n+1}\|^2 \\
& \leq \frac{\Delta t C_r C_{PF,2}^2}{\epsilon_1} \|\zeta_t\|_{L^\infty(t^n, t^{n+1}; L^2(\Omega))}^2 + \frac{\Delta t \epsilon_1}{r} \|\nabla \psi_h^{n+1}\|^2 + \frac{C_r \kappa^2 \Delta t}{\epsilon_2} \|\nabla \zeta^{n+1}\|^2 + \frac{\Delta t \epsilon_2}{r} \|\nabla \psi_h^{n+1}\|^2 \\
& + \frac{C_3^2 C_r \Delta t}{\epsilon_3} \|\nabla u^{n+1}\|^2 \|\nabla \zeta^{n+1}\|^2 + \frac{\Delta t \epsilon_3}{r} \|\nabla \psi_h^{n+1}\|^2 + \frac{C_r C_3^2 \Delta t^3}{\epsilon_4} \|\nabla T_h^{n+1}\|^2 \|\nabla u_t\|_{L^\infty(t^n, t^{n+1}; L^2(\Omega))}^2 \\
& + \frac{\Delta t \epsilon_4}{r} \|\nabla \psi_h^{n+1}\|^2 + \frac{C_r C_3^2 \Delta t}{\epsilon_5} \|\nabla \eta^n\|^2 \|\nabla T_h^{n+1}\|^2 + \frac{\Delta t \epsilon_5}{r} \|\nabla \psi_h^{n+1}\|^2 + \frac{C_4 C_T \Delta t \epsilon_6}{2} \|\nabla \psi_h^{n+1}\|^2 \\
& + \frac{C_4 C_T \Delta t \delta_6}{4 \epsilon_6} \|\nabla \phi_h^n\|^2 + \frac{C_4 C_T \Delta t}{4 \epsilon_6 \delta_6} \|\phi_h^n\|^2 + \frac{C_r C_3^2 \Delta t}{\epsilon_7} \|\nabla u_h^n\|^2 \|\nabla \zeta^{n+1}\|^2 + \frac{\Delta t \epsilon_7}{r} \|\nabla \psi_h^{n+1}\|^2 \\
& + \frac{C_r C_3^2 \Delta t}{\epsilon_8} \|\nabla u_h^n\|^2 \|\nabla \zeta^n\|^2 + \frac{\Delta t \epsilon_8}{r} \|\nabla \psi_h^{n+1}\|^2 + \frac{C_6^2 C_{inv,2} \Delta t^2}{h \epsilon_9} \|\nabla u_h^n\|^2 \|\nabla \psi_h^{n+1}\|^2 + \frac{\epsilon_9}{2} \|\psi_h^{n+1} - \psi_h^n\|^2 \\
& + \frac{C_r C_3^2 \Delta t^3}{\epsilon_{10}} \|\nabla u_h^n\|^2 \|\nabla T_t\|_{L^\infty(t^n, t^{n+1}; L^2(\Omega))}^2 + \frac{\Delta t \epsilon_{10}}{r} \|\nabla \psi_h^{n+1}\|^2 \\
& + \frac{C_{PF,2}^2 C_r \Delta t^3}{\epsilon_{11}} \|T_{tt}\|_{L^\infty(t^n, t^{n+1}; L^2(\Omega))}^2 + \frac{\epsilon_{11}}{r} \|\nabla \psi_h^{n+1}\|^2,
\end{aligned}$$

and

$$\begin{aligned}
(78) \quad & \frac{1}{2} \left\{ \|\phi_h^{n+1}\|^2 - \|\phi_h^n\|^2 + \|\phi_h^{n+1} - \phi_h^n\|^2 \right\} + Pr \Delta t \|\nabla \phi_h^{n+1}\|^2 \\
& \leq \frac{\Delta t C_r C_{PF,1}^2}{\epsilon_{12}} \|\eta_t\|_{L^\infty(t^n, t^{n+1}; L^2(\Omega))}^2 + \frac{\Delta t \epsilon_{12}}{r} \|\nabla \phi_h^{n+1}\|^2 + \frac{C_r Pr^2 \Delta t}{\epsilon_{13}} \|\nabla \eta^{n+1}\|^2 \\
& + \frac{\Delta t \epsilon_{13}}{r} \|\nabla \phi_h^{n+1}\|^2 + \frac{d C_r \Delta t}{\epsilon_{14}} \|p^{n+1} - q_h^{n+1}\|^2 + \frac{\Delta t \epsilon_{14}}{r} \|\nabla \phi_h^{n+1}\|^2 \\
& + \Delta t Pr^2 Ra^2 C_{PF,1}^2 C_{PF,2}^2 C_r \left(\frac{1}{\epsilon_{15}} \|\nabla \zeta^{n+1}\|^2 + \frac{1}{\epsilon_{16}} \|\nabla \psi_h^{n+1}\|^2 \right) + \frac{\Delta t}{r} \left(\frac{1}{\epsilon_{15}} \|\nabla \phi_h^{n+1}\|^2 + \frac{1}{\epsilon_{16}} \|\nabla \phi_h^{n+1}\|^2 \right) \\
& + \frac{C_1 C_r \Delta t}{\epsilon_{17}} \|\nabla u^{n+1}\|^2 \|\nabla \eta^{n+1}\|^2 + \frac{\Delta t \epsilon_{17}}{r} \|\nabla \phi_h^{n+1}\|^2 \\
& + \frac{C_r C_1^2 \Delta t^3}{\epsilon_{18}} \|\nabla u_h^{n+1}\|^2 \|\nabla u_t\|_{L^\infty(t^n, t^{n+1}; L^2(\Omega))}^2 + \frac{\Delta t \epsilon_{18}}{r} \|\nabla \phi_h^{n+1}\|^2 + \frac{C_r C_1 \Delta t}{\epsilon_{19}} \|\nabla \eta^n\|^2 \|\nabla u_h^{n+1}\|^2 \\
& + \frac{\Delta t \epsilon_{19}}{r} \|\nabla \phi_h^{n+1}\|^2 + \frac{C_2 C_u \Delta t \epsilon_{20}}{2} \|\nabla \phi_h^{n+1}\|^2 + \frac{C_2 C_u \Delta t \delta_{20}}{4 \epsilon_{20}} \|\nabla \phi_h^n\|^2 + \frac{C_2 C_u \Delta t}{4 \epsilon_{20} \delta_{20}} \|\phi_h^n\|^2 \\
& + \frac{C_r C_1^2 \Delta t}{\epsilon_{21}} \|\nabla u_h^n\|^2 \|\nabla \eta^{n+1}\|^2 + \frac{\Delta t \epsilon_{21}}{r} \|\nabla \phi_h^{n+1}\|^2 + \frac{C_r C_1 \Delta t}{\epsilon_{22}} \|\nabla u_h^n\|^2 \|\nabla \eta^n\|^2 + \frac{\Delta t \epsilon_{22}}{r} \|\nabla \phi_h^{n+1}\|^2 \\
& + \frac{C_5^2 C_{inv,1} \Delta t^2}{h \epsilon_{23}} \|\nabla u_h^n\|^2 \|\nabla \phi_h^{n+1}\|^2 + \frac{\epsilon_{23}}{2} \|\phi_h^{n+1} - \phi_h^n\|^2 + \frac{C_r C_1 \Delta t^3}{\epsilon_{24}} \|\nabla u_h^n\|^2 \|\nabla u_t\|_{L^\infty(t^n, t^{n+1}; L^2(\Omega))}^2 \\
& + \frac{\Delta t \epsilon_{24}}{r} \|\nabla \phi_h^{n+1}\|^2 + \frac{C_{PF,1}^2 C_r \Delta t^3}{\epsilon_{26}} \|u_{tt}\|_{L^\infty(t^n, t^{n+1}; L^2(\Omega))}^2 + \frac{\Delta \epsilon_{26}}{r} \|\nabla \phi_h^{n+1}\|^2.
\end{aligned}$$

Combine (77) and (78), choose free parameters appropriately, use condition (31), and take the maximum

over all constants on the r.h.s. Then,

$$\begin{aligned}
(79) \quad & \frac{1}{2} (\|\psi_h^{n+1}\|^2 - \|\psi_h^n\|^2) + \frac{1}{4} \|\psi_h^{n+1} - \psi_h^n\|^2 + \frac{\kappa \Delta t}{4} (\|\nabla \psi_h^{n+1}\|^2 - \|\nabla \psi_h^n\|^2) \\
& + \frac{1}{2} (\|\phi_h^{n+1}\|^2 - \|\phi_h^n\|^2) + \frac{1}{4} \|\phi_h^{n+1} - \phi_h^n\|^2 + \frac{Pr \Delta t}{4} (\|\nabla \phi_h^{n+1}\|^2 - \|\nabla \phi_h^n\|^2) \\
& \leq C \left\{ \Delta t \|\zeta_t\|_{L^\infty(t^n, t^{n+1}; L^2(\Omega))}^2 + \Delta t \|\nabla \zeta^{n+1}\|^2 + \Delta t \|\nabla u^{n+1}\|^2 \|\nabla \zeta^{n+1}\|^2 \right. \\
& + \Delta t^3 \|\nabla T_h^{n+1}\|^2 \|\nabla u_t\|_{L^\infty(t^n, t^{n+1}; L^2(\Omega))}^2 + \Delta t \|\nabla \eta^n\|^2 \|\nabla T_h^{n+1}\|^2 + \Delta t \|\phi_h^n\|^2 + \Delta t \|\nabla u_h'^n\|^2 \|\nabla \zeta^{n+1}\|^2 \\
& + \Delta t \|\nabla u_h'^n\|^2 \|\nabla \zeta^n\|^2 + \Delta t^3 \|\nabla u_h'^n\|^2 \|\nabla T_t\|_{L^\infty(t^n, t^{n+1}; L^2(\Omega))}^2 + \Delta t^3 \|T_{tt}\|_{L^\infty(t^n, t^{n+1}; L^2(\Omega))}^2 \\
& + \Delta t \|p^{n+1} - q_h^{n+1}\|^2 + \Delta t \|\eta_t\|_{L^\infty(t^n, t^{n+1}; L^2(\Omega))}^2 + \Delta t \|\nabla \eta^{n+1}\|^2 + \Delta t \|\nabla \zeta^{n+1}\|^2 \\
& + \Delta t \|\nabla u^{n+1}\|^2 \|\nabla \eta^{n+1}\|^2 + \Delta t^3 \|\nabla u_h^{n+1}\|^2 \|\nabla u_t\|_{L^\infty(t^n, t^{n+1}; L^2(\Omega))}^2 + \Delta t \|\nabla \eta^n\|^2 \|\nabla u_h^{n+1}\|^2 \\
& + \Delta t \|\nabla u_h^n\|^2 \|\nabla \eta^{n+1}\|^2 + \Delta t \|\nabla u_h'^n\|^2 \|\nabla \eta^n\|^2 + \Delta t^3 \|\nabla u_h'^n\|^2 \|\nabla u_t\|_{L^\infty(t^n, t^{n+1}; L^2(\Omega))}^2 \\
& \left. + \Delta t^3 \|u_{tt}\|_{L^\infty(t^n, t^{n+1}; L^2(\Omega))}^2 \right\}.
\end{aligned}$$

Multiply by 2, sum from $n = 0$ to $n = N - 1$, apply Lemma 3, and renorm. Then,

$$\begin{aligned}
& \|\psi_h^N\|^2 + \|\phi_h^N\|^2 + \frac{1}{2} \sum_{n=0}^{N-1} (\|\psi_h^{n+1} - \psi_h^n\|^2 + \|\phi_h^{n+1} - \phi_h^n\|^2) + \frac{\kappa \Delta t}{2} \|\nabla \psi_h^N\|^2 + \frac{Pr \Delta t}{2} \|\nabla \phi_h^N\|^2 \\
& \leq C \left\{ (2 + \|\nabla u^{n+1}\|^2 + 2 \|\nabla u_h'^n\|^2) \Delta t \|\nabla \zeta\|_{\infty,0}^2 + (1 + \|\nabla T_h^{n+1}\|^2 + \|\nabla u^{n+1}\|^2 + \|\nabla u_h^{n+1}\|^2 + 2 \|\nabla u_h'^n\|^2) \Delta t \|\nabla \eta\|_{\infty,0}^2 \right. \\
& + \Delta t \|\zeta_t\|_{\infty,0}^2 + (\|\nabla T_h^{n+1}\|^2 + \|\nabla u_h^{n+1}\|^2 + \|\nabla u_h'^n\|^2) \Delta t^3 \|\nabla u_t\|_{\infty,0}^2 + \Delta t^3 \|\nabla u_h'^n\|^2 \|\nabla T_t\|_{\infty,0}^2 + \Delta t^3 \|T_{tt}\|_{2,0}^2 \\
& + \Delta t \|p - q_h\|_{\infty,0}^2 + \Delta t \|\eta_t\|_{\infty,0}^2 + \Delta t^3 \|u_{tt}\|_{\infty,0}^2 \left. \right\} + \|\psi_h^0\|^2 + \frac{\kappa \Delta t}{2} \|\nabla \psi_h^0\|^2 + \|\phi_h^0\|^2 + \frac{Pr \Delta t}{2} \|\nabla \phi_h^0\|^2 \\
& \leq C \left\{ \Delta t \|\nabla \zeta\|_{\infty,0}^2 + \Delta t \|\nabla \eta\|_{\infty,0}^2 + \Delta t \|\zeta_t\|_{\infty,0}^2 + \Delta t^3 \|\nabla u_t\|_{\infty,0}^2 + \Delta t^3 \|\nabla T_t\|_{\infty,0}^2 \right. \\
& + \Delta t \|p - q_h\|_{\infty,0}^2 + \Delta t \|\eta_t\|_{\infty,0}^2 + \Delta t^3 \|u_{tt}\|_{\infty,0}^2 \left. \right\} + \|\psi_h^0\|^2 + \frac{\kappa \Delta t}{2} \|\nabla \psi_h^0\|^2 + \|\phi_h^0\|^2 + \frac{Pr \Delta t}{2} \|\nabla \phi_h^0\|^2.
\end{aligned}$$

Take infimums over X_h , Q_h , and W_h . Apply the triangle inequality, then

$$\begin{aligned}
& \|e_T^N\|^2 + \|e_u^N\|^2 + \frac{1}{2} \sum_{n=0}^{N-1} (\|e_T^{n+1} - e_T^n\|^2 + \|e_u^{n+1} - e_u^n\|^2) + \frac{\kappa \Delta t}{2} \|\nabla e_T^N\|^2 + \frac{Pr \Delta t}{2} \|\nabla e_u^N\|^2 \\
& \leq C \left\{ \Delta t \inf_{v_h \in X_h} \left(\|\nabla(u - v_h)\|_{\infty,0}^2 + \|(u - v_h)_t\|_{\infty,0}^2 \right) + \Delta t \inf_{S_h \in W_h} \left(\|\nabla(T - S_h)\|_{\infty,0}^2 + \|(T - S_h)_t\|_{\infty,0}^2 \right) \right. \\
& \quad + \Delta t \inf_{q_h \in Q_h} \|p - q_h\|_{\infty,0}^2 + \Delta t^3 + \Delta t \|\nabla \eta^0\|^2 + \Delta t \|\nabla \zeta^0\|^2 + \|\eta^0\|^2 \\
& \quad \left. + \|\zeta^0\|^2 + \|e_T^0\|^2 + \|e_u^0\|^2 + \Delta t \|\nabla e_T^0\|^2 + \Delta t \|\nabla e_u^0\|^2 \right\}. \quad \square
\end{aligned}$$

The same result holds, with a different constant, for the thin wall problem.

THEOREM 9. For (u, p, T) satisfying (9) - (13), suppose that $(u_h^0, p_h^0, T_h^0) \in (X_h, Q_h, W_h)$ are approximations of (u^0, p^0, T^0) to within the accuracy of the interpolant. Further, suppose that condition (31) holds. Then there exists a constant C such that

$$\begin{aligned}
& \|e_T^N\|^2 + \|e_u^N\|^2 + \frac{1}{2} \sum_{n=0}^{N-1} (\|e_T^{n+1} - e_T^n\|^2 + \|e_u^{n+1} - e_u^n\|^2) + \frac{\kappa \Delta t}{2} \|\nabla e_T^N\|^2 + \frac{Pr \Delta t}{2} \|\nabla e_u^N\|^2 \\
& \leq C \left\{ \Delta t \inf_{v_h \in X_h} \left(\|\nabla(u - v_h)\|_{\infty,0}^2 + \|(u - v_h)_t\|_{\infty,0}^2 \right) + \Delta t \inf_{S_h \in W_h} \left(\|\nabla(T - S_h)\|_{\infty,0}^2 + \|(T - S_h)_t\|_{\infty,0}^2 \right) \right. \\
& \quad + \Delta t \inf_{q_h \in Q_h} \|p - q_h\|_{\infty,0}^2 + \Delta t^3 + \Delta t \|\nabla \eta^0\|^2 + \Delta t \|\nabla \zeta^0\|^2 + \|\eta^0\|^2 \\
& \quad \left. + \|\zeta^0\|^2 + \|e_T^0\|^2 + \|e_u^0\|^2 + \Delta t \|\nabla e_T^0\|^2 + \Delta t \|\nabla e_u^0\|^2 \right\}.
\end{aligned}$$

Proof. We follow the same methodology as in Theorem 8. The error equations for velocity and temperature are

$$(80) \quad \left(\frac{e_u^{n+1} - e_u^n}{\Delta t}, v_h \right) - b(u_h^n - u_h'^n, u_h^{n+1}, v_h) - b(u_h'^n, u_h^n, v_h) + Pr(\nabla e_u^{n+1}, \nabla v_h) - (e_p^{n+1}, \nabla \cdot v_h) \\ = PrRa \left\{ (\gamma T^{n+1}, v_h) - (\gamma T_h^n, v_h) \right\} + \tau_u(u^{n+1}, v_h) \quad \forall v_h \in X_h,$$

$$(81) \quad \left(\frac{e_T^{n+1} - e_T^n}{\Delta t}, S_h \right) + b^*(u^{n+1}, T^{n+1}, S_h) - b^*(u_h^n - u_h'^n, T_h^n, S_h) - b^*(u_h'^n, T_h^n, S_h) + \kappa(\nabla e_T^{n+1}, \nabla S_h) \\ = (u_1^{n+1}, S_h) - (u_{1h}^n, S_h) + \tau_T(T^{n+1}, S_h) \quad \forall S_h \in W_h.$$

Add and subtract $PrRa(\gamma T^n, v_h)$ in (80) and (u_1^n, S_h) in (81). Then,

$$(82) \quad \left(\frac{e_u^{n+1} - e_u^n}{\Delta t}, v_h \right) - b(u_h^n - u_h'^n, u_h^{n+1}, v_h) - b(u_h'^n, u_h^n, v_h) + Pr(\nabla e_u^{n+1}, \nabla v_h) - (e_p^{n+1}, \nabla \cdot v_h) \\ = PrRa \left\{ (\gamma(T^{n+1} - T^n), v_h) - (\gamma e_T^n, v_h) \right\} + \tau_u(u^{n+1}, v_h) \quad \forall v_h \in X_h,$$

$$(83) \quad \left(\frac{e_T^{n+1} - e_T^n}{\Delta t}, S_h \right) + b^*(u^{n+1}, T^{n+1}, S_h) - b^*(u_h^n - u_h'^n, T_h^n, S_h) - b^*(u_h'^n, T_h^n, S_h) + \kappa(\nabla e_T^{n+1}, \nabla S_h) \\ = (u_1^{n+1} - u_1^n, S_h) - (e_{u1}^n, S_h) + \tau_T(T^{n+1}, S_h) \quad \forall S_h \in W_h.$$

Estimate the new terms using similar techniques as in Theorem 8:

$$(84) \quad |PrRa(\gamma(T^{n+1} - T^n), v_h)| \leq \frac{Pr^2 Ra^2 C_{PF,1}^2 C_r}{\epsilon_{26}} \|T^{n+1} - T^n\|^2 + \frac{\epsilon_{26}}{r} \|\nabla v_h\|^2 \\ \leq \frac{Pr^2 Ra^2 C_{PF,1}^2 C_r \Delta t^2}{\epsilon_{26}} \|T_t\|_{L^\infty(t^n, t^{n+1}; L^2(\Omega))}^2 + \frac{\epsilon_{26}}{r} \|\nabla v_h\|^2,$$

$$(85) \quad |PrRa(\gamma e_T^n, v_h)| = |PrRa(\gamma \zeta^n, v_h) - PrRa(\gamma \psi_h^n, v_h)| \\ \leq \frac{Pr^2 Ra^2 C_{PF,1}^2 C_r}{\epsilon_{27}} (\|\zeta^n\|^2 + \|\psi_h^n\|^2) + \frac{2\epsilon_{27}}{r} \|\nabla v_h\|^2,$$

$$(86) \quad |(u_1^{n+1} - u_1^n, S_h)| \leq \frac{C_{PF,2}^2 C_r}{\epsilon_{28}} \|u_1^{n+1} - u_1^n\|^2 + \frac{\epsilon}{r} \|\nabla S_h\|^2 \\ \leq \frac{C_{PF,2}^2 C_r \Delta t^2}{\epsilon_{28}} \|u_t\|_{L^\infty(t^n, t^{n+1}; L^2(\Omega))}^2 + \frac{\epsilon_{28}}{r} \|\nabla S_h\|^2,$$

$$(87) \quad |(e_{u1}^n, S_h)| = |(\eta_1^n, S_h) - (\phi_{1h}^n, S_h)| \leq \frac{Pr^2 Ra^2 C_{PF,1}^2 C_r}{\epsilon_{29}} (\|\eta^n\|^2 + \|\phi_h^n\|^2) + \frac{2\epsilon_{29}}{r} \|\nabla S_h\|^2.$$

Apply estimates similar to those in Theorem 8 as well as the above estimates, multiply by $2\Delta t$, sum from $n = 0$ to $n = N - 1$. Further, apply Lemma 3, triangle inequality and arrive at the result. \square

COROLLARY 10. *Suppose the assumptions of Theorem 4 hold. Further suppose that the finite element spaces (X_h, Q_h, W_h) are given by P2-P1-P2 (Taylor-Hood), then the errors in velocity and temperature satisfy*

$$\|e_T^N\|^2 + \|e_u^N\|^2 + \frac{1}{2} \sum_{n=0}^{N-1} (\|e_T^{n+1} - e_T^n\|^2 + \|e_u^{n+1} - e_u^n\|^2) + \frac{\kappa \Delta t}{2} \|\nabla e_T^N\|^2 + \frac{Pr \Delta t}{2} \|\nabla e_u^N\|^2 \\ \leq C(\Delta t h^4 + \Delta t h^6 + \Delta t^3 + \Delta t \|\nabla \eta^0\|^2 + \Delta t \|\nabla \zeta^0\|^2 + \|\eta^0\|^2 \\ + \|\zeta^0\|^2 + \|e_T^0\|^2 + \|e_u^0\|^2 + \Delta t \|\nabla e_T^0\|^2 + \Delta t \|\nabla e_u^0\|^2).$$

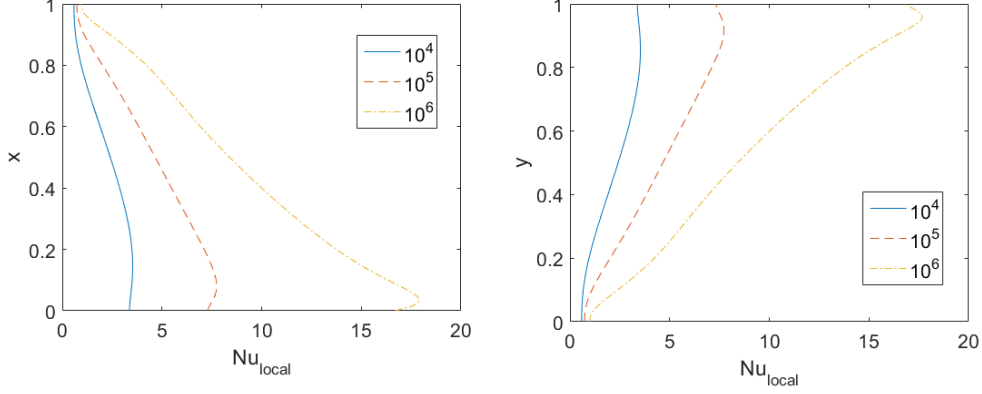


Fig. 2: Variation of the local Nusselt number at the hot (left) and cold walls (right).

COROLLARY 11. *Suppose the assumptions of Theorem 4 hold. Further suppose that the finite element spaces (X_h, Q_h, W_h) are given by P1b-P1-P1b (MINI element), then the errors in velocity and temperature satisfy*

$$\begin{aligned} \|e_T^N\|^2 + \|e_u^N\|^2 + \frac{1}{2} \sum_{n=0}^{N-1} (\|e_T^{n+1} - e_T^n\|^2 + \|e_u^{n+1} - e_u^n\|^2) + \frac{\kappa \Delta t}{2} \|\nabla e_T^N\|^2 + \frac{Pr \Delta t}{2} \|\nabla e_u^N\|^2 \\ \leq C(\Delta t h^2 + \Delta t h^4 + \Delta t^3 + \Delta t \|\nabla \eta^0\|^2 + \Delta t \|\nabla \zeta^0\|^2 + \|\eta^0\|^2 \\ + \|\zeta^0\|^2 + \|e_T^0\|^2 + \|e_u^0\|^2 + \Delta t \|\nabla e_T^0\|^2 + \Delta t \|\nabla e_u^0\|^2). \end{aligned}$$

5. Numerical Experiments. In this section, we illustrate the stability and convergence of the numerical scheme described by (28) - (30) using Taylor-Hood (P2-P1-P2) elements to approximate the average velocity, pressure, and temperature. The numerical experiments include the double pane window benchmark problem of de Vahl Davis [19], a convergence experiment and predictability exploration with an analytical solution adopted from [22] devised through the method of manufactured solutions. The software used for all tests is FREEFEM++ [9].

5.1. Stability condition. The constant appearing in condition (31) is estimated by pre-computations for the double pane window problem appearing below. We set $C_\dagger = 1$. The first condition is used and checked at each iteration. If violated, the timestep is halved and the iteration is repeated. The timestep is never increased. The condition is violated three times during the computation of the double pane window problem with $Ra = 10^6$ in Section 5.3.

5.2. Perturbation generation. The bred vector (BV) algorithm of Toth and Kalnay [18] is used to generate perturbations in the double pane window problem and in exploring predictability. The BV algorithm produces a perturbation with maximal separation rate. We set $J = 2$ and $d = 2$ in all experiments. An initial random positive/negative perturbation pair was generated $\pm \epsilon = \pm(\epsilon_1, \epsilon_2, \epsilon_3)$ with $\epsilon_i \in (0, 0.01) \forall i = 1, 2, 3$; that is, a pair of initial perturbations for each component of velocity and temperature. Utilizing the scheme (28) - (30), denote the control and perturbed numerical approximations χ_h^n and $\chi_{p,h}^n$, respectively. Then, a bred vector $bv(\chi; \epsilon_i)$ is generated via:

Step one: Given χ_h^0 and ϵ_i , put $\chi_{p,h}^0 = \chi_h^0 + \epsilon_i$. Select time reinitialization interval $\delta t \geq \Delta t$ and let $t^k = k\delta t$ with $0 \leq k \leq k^* \leq N$.

Step two: Compute χ_h^k and $\chi_{p,h}^k$. Calculate $bv(\chi^k; \epsilon_i) = \frac{\epsilon_i}{\|\chi_{p,h}^k - \chi_h^k\|} (\chi_{p,h}^k - \chi_h^k)$.

Step three: Put $\chi_{p,h}^k = \chi_h^k + bv(\chi^k; \epsilon_i)$.

Step four: Repeat **Step two** with $k = k + 1$.

Step five: Put $bv(\chi; \epsilon_i) = bv(\chi^{k^*}; \epsilon_i)$.

A positive/negative perturbed initial condition pair is generated via $\chi_\pm = \chi^0 + bv(\chi; \pm \epsilon_i)$. We let $\delta t = \Delta t = 0.001$ and $k^* = 5$.

5.3. The double pane window problem. The first numerical experiment is the benchmark problem of de Vahl Davis [19]. The problem is the two-dimensional flow of a fluid in an unit square cavity with $Pr = 0.71$ and $\kappa = 1.0$. Both velocity components (i.e. $u = 0$) are zero on the boundaries. The horizontal walls are insulated and the left and right vertical walls are maintained at temperatures $T(0, y, t) = 1$ and $T(1, y, t) = 0$, respectively; see Figure 1b. We let $10^3 \leq Ra \leq 10^6$. The initial conditions for velocity and temperature are generated via the BV algorithm in Section 5.2,

$$\begin{aligned} u_{\pm}(x, y, 0) &:= u(x, y, 0; \omega_{1,2}) = (1 + bv(u; \pm\epsilon_1), 1 + bv(u; \pm\epsilon_2))^T, \\ T_{\pm}(x, y, 0) &:= T(x, y, 0; \omega_{1,2}) = 1 + bv(T; \pm\epsilon_3). \end{aligned}$$

Both $f(x, t; \omega_j)$ and $g(x, t; \omega_j)$ are identically zero for $j = 1, 2$. The finite element mesh is a division of $[0, 1]^2$ into 64^2 squares with diagonals connected with a line within each square in the same direction. The stopping condition is

$$\max_{0 \leq n \leq N-1} \left\{ \frac{\|u_h^{n+1} - u_h^n\|}{\|u_h^{n+1}\|}, \frac{\|T_h^{n+1} - T_h^n\|}{\|T_h^{n+1}\|} \right\} \leq 10^{-5}$$

and initial timestep $\Delta t = 0.001$. The timestep was halved three times to 0.000125 to maintain stability for $Ra = 10^6$. Several quantities are compared with benchmark solutions in the literature. These include the maximum vertical velocity at $y = 0.5$, $\max_{x \in \Omega_h} u_2(x, 0.5, t^*)$, and maximum horizontal velocity at $x = 0.5$, $\max_{y \in \Omega_h} u_1(0.5, y, t^*)$. We present our computed values for the mean flow in Tables 1 and 2 alongside several of those seen in the literature. Furthermore, the local Nusselt number is calculated at the cold (+) and hot walls (-), respectively, via

$$Nu_{local} = \pm \frac{\partial T}{\partial x}.$$

The average Nusselt number on the vertical boundary at $x = 0$ is calculated via

$$Nu_{avg} = \int_0^1 Nu_{local} dy.$$

Figure 2 presents the plots of Nu_{local} at the hot and cold walls. Table 3 presents computed values of Nu_{avg} alongside several of those seen in the literature. Figures 3 and 4 present the velocity streamlines and temperature isotherms for the averages. All results are seen to be in good agreement with the benchmark values in the literature [4, 15, 19, 20, 22].

Ra	Present study	Ref. [19]	Ref. [15]	Ref. [20]	Ref. [4]	Ref. [22]
10^4	16.18 (64×64)	16.18 (41×41)	16.10 (71×71)	16.10 (101×101)	15.90 (11×11)	16.18 (64×64)
10^5	34.72 (64×64)	34.81 (81×81)	34 (71×71)	34 (101×101)	33.51 (21×21)	34.74 (64×64)
10^6	64.80 (64×64)	65.33 (81×81)	65.40 (71×71)	65.40 (101×101)	65.52 (32×32)	64.81 (64×64)

Table 1: Comparison of maximum horizontal velocity at $x = 0.5$ together with mesh size used in computation for the double pane window problem.

Ra	Present study	Ref. [19]	Ref. [15]	Ref. [20]	Ref. [4]	Ref. [22]
10^4	19.60 (64×64)	19.51 (41×41)	19.90 (71×71)	19.79 (101×101)	19.91 (11×11)	19.62 (64×64)
10^5	68.53 (64×64)	68.22 (81×81)	70 (71×71)	70.63 (101×101)	70.60 (21×21)	68.48 (64×64)
10^6	215.96 (64×64)	216.75 (81×81)	228 (71×71)	227.11 (101×101)	228.12 (32×32)	220.44 (64×64)

Table 2: Comparison of maximum horizontal velocity at $y = 0.5$ together with mesh size used in computation for the double pane window problem.

Ra	Present study	Ref. [19]	Ref. [15]	Ref. [20]	Ref. [4]	Ref. [22]
10^4	2.24 (64×64)	2.24 (41×41)	2.08 (71×71)	2.25 (101×101)	2.15 (11×11)	2.25 (64×64)
10^5	4.52 (64×64)	4.52 (81×81)	4.30 (71×71)	4.59 (101×101)	4.35 (21×21)	4.53 (64×64)
10^6	8.87 (64×64)	8.92 (81×81)	8.74 (71×71)	8.97 (101×101)	8.83 (32×32)	8.87 (64×64)

Table 3: Comparison of average Nusselt number on the vertical boundary at $x = 0$ together with mesh size used in computation for the double pane window problem.

5.4. Numerical convergence study. In this section, we illustrate the convergence rates for the proposed algorithm (28) - (30). The unperturbed solution is given by

$$\begin{aligned} u(x, y, t) &= (10x^2(x-1)^2y(y-1)(2y-1)\cos(t), -10x(x-1)(2x-1)y^2(y-1)^2\cos(t))^T, \\ T(x, y, t) &= u_1(x, y, t) + u_2(x, y, t), \\ p(x, y, t) &= 10(2x-1)(2y-1)\cos(t), \end{aligned}$$

with $\kappa = Pr = 1.0$, $Ra = 100$, and $\Omega = [0, 1]^2$. The perturbed solutions are given by

$$\begin{aligned} u(x, y, t; \omega_{1,2}) &= (1 + \epsilon_{1,2})u(x, y, t), \\ T(x, y, t; \omega_{1,2}) &= (1 + \epsilon_{1,2})T(x, y, t), \\ p(x, y, t; \omega_{1,2}) &= (1 + \epsilon_{1,2})p(x, y, t), \end{aligned}$$

where $\epsilon_1 = 1e - 2 = -\epsilon_2$ and both forcing and boundary terms are adjusted appropriately. The perturbed solutions satisfy the following relations,

$$\begin{aligned} \langle u \rangle &= 0.5(u(x, y, t; \omega_1) + u(x, y, t; \omega_2)) = u(x, y, t), \\ \langle T \rangle &= 0.5(T(x, y, t; \omega_1) + T(x, y, t; \omega_2)) = T(x, y, t), \\ \langle p \rangle &= 0.5(p(x, y, t; \omega_1) + p(x, y, t; \omega_2)) = p(x, y, t). \end{aligned}$$

The finite element mesh is a Delaunay triangulation generated from m points on each side of Ω . We calculate errors in the approximations of the average velocity, temperature and pressure with the $L^\infty(0, t^*; L^2(\Omega))$ and $L^\infty(0, t^*; H^1(\Omega))$ norms. Rates are calculated from the errors at two successive $m_{1,2}$ or $\Delta t_{1,2}$ via

$$\begin{aligned} &\frac{\log_2(e_\chi(m_1)/e_\chi(m_2))}{\log_2(m_1/m_2)}, \\ &\frac{\log_2(e_\chi(\Delta t_1)/e_\chi(\Delta t_2))}{\log_2(\Delta t_1/\Delta t_2)}, \end{aligned}$$

respectively, with $\chi = u, T, p$. We first illustrate spatial convergence. We isolate the spatial error by first choosing a fixed timestep $\Delta t = 0.0001$ and setting the final time $t^* = 0.001$. The parameter m is varied between 4, 8, 16, 32, 64, and 128. Results are presented in Table 4. Third order convergence is observed in velocity and temperature and second order convergence in pressure in the $L^\infty(0, t^*; L^2(\Omega))$ norm and second order convergence in velocity and temperature in the $L^\infty(0, t^*; H^1(\Omega))$ norm.

Temporal convergence is illustrated by choosing a fixed $m = 64$ and setting the final time $t^* = 1$. The timestep is varied between 4, 8, 16, 32, 64, 128. Table 5 confirms first order convergence in velocity, temperature, and pressure in the $L^\infty(0, t^*; L^2(\Omega))$ norm and in velocity and temperature in the $L^\infty(0, t^*; H^1(\Omega))$ norm.

$1/m$	$\ \langle u_h \rangle - \langle u \rangle \ _{\infty,0}$	Rate	$\ \nabla \langle u_h \rangle - \nabla u \ _{\infty,0}$	Rate	$\ \langle T_h \rangle - \langle T \rangle \ _{\infty,0}$	Rate	$\ \nabla \langle T_h \rangle - \nabla T \ _{\infty,0}$	Rate	$\ \langle p_h \rangle - \langle p \rangle \ _{\infty,0}$	Rate
4	0.00134087	-	0.0376324	-	2.49E-04	-	0.0100481	-	0.427751	-
8	3.68E-04	1.87	0.0162059	1.22	3.03E-05	3.04	0.00171527	2.55	0.0256596	4.06
16	5.56E-05	2.73	0.00443669	1.87	4.95E-06	2.61	4.82E-04	1.83	0.00482023	2.41
32	6.35E-06	3.13	9.80E-04	2.18	5.71E-07	3.12	1.07E-04	2.18	1.10E-03	2.13
64	8.67E-07	2.87	2.70E-04	1.86	8.13E-08	2.81	3.01E-05	1.82	2.70E-04	2.02
128	1.06E-07	3.04	6.63E-05	2.03	9.56E-09	3.09	7.08E-06	2.09	6.58E-05	2.04

Table 4: Errors and rates for average velocity, temperature, and pressure in corresponding norms.

$1/\Delta t$	$\ \langle u_h \rangle - \langle u \rangle \ _{\infty,0}$	Rate	$\ \nabla \langle u_h \rangle - \nabla u \ _{\infty,0}$	Rate	$\ \langle T_h \rangle - \langle T \rangle \ _{\infty,0}$	Rate	$\ \nabla \langle T_h \rangle - \nabla T \ _{\infty,0}$	Rate	$\ \langle p_h \rangle - \langle p \rangle \ _{\infty,0}$	Rate
4	0.00698068	-	0.0524076	-	1.12E-04	-	0.000798053	-	0.122182	-
8	0.0036989	0.92	0.0277725	0.92	6.78E-05	0.73	4.81E-04	0.73	0.0647005	0.92
16	0.001898	0.96	0.0142518	0.96	3.66E-05	0.89	2.60E-04	0.89	0.0331928	0.96
32	9.61E-04	0.98	0.00721454	0.98	1.89E-05	0.95	1.35E-04	0.94	0.0168049	0.98
64	4.83E-04	0.99	0.00363088	0.99	9.62E-06	0.98	7.02E-05	0.95	0.00846082	0.99
128	2.42E-04	1.00	0.00182511	0.99	4.85E-06	0.99	3.81E-05	0.89	0.0042531	0.99

Table 5: Errors and rates for average velocity, temperature, and pressure in corresponding norms.

5.5. Exploration of predictability. Consider the problem with manufactured solution in Section 5.4. However, instead of specifying the perturbations on the initial conditions, the BV algorithm in Section 5.2 yields

$$\begin{aligned} u_{\pm}(x, y, 0) &:= u(x, y, 0; \omega_{1,2}) = (u_1(x, y, 0) + bv(u; \pm\epsilon_1), u_2(x, y, 0) + bv(u; \pm\epsilon_2))^T, \\ T_{\pm}(x, y, 0) &:= T(x, y, 0; \omega_{1,2}) = T(x, y, 0) + bv(T; \pm\epsilon_3). \end{aligned}$$

The forcing functions and boundary conditions are left unperturbed. Further, the Rayleigh number is varied between 10^2 and 10^4 . The initial timestep is 0.001 and final time $t^* = 0.5$. Herein, we will define energy, variance, average effective Lyapunov exponent [2], and δ -predictability horizon [2].

DEFINITION 12. *The energy is given by*

$$\text{Energy} := \|T\| + \frac{1}{2}\|u\|^2.$$

The variance of χ is

$$V(\chi) := \langle \|\chi\|^2 \rangle - \langle \chi \rangle^2 = \langle \|\chi'\|^2 \rangle.$$

The relative energy fluctuation is

$$r(t) := \frac{\|\chi_+ - \chi_-\|^2}{\|\chi_+\|\|\chi_-\|},$$

and the average effective Lyapunov exponent over $0 < \tau \leq t^$ is*

$$\gamma_{\tau}(t) := \frac{1}{2\tau} \log \left(\frac{r(t+\tau)}{r(t)} \right),$$

with $0 < t + \tau \leq t^$. The δ -predictability horizon is*

$$t_p := \frac{1}{\gamma_{t^*}(0)} \log \left(\frac{\delta}{\|(\chi_+ - \chi_-)(0)\|} \right).$$

Figure 3 presents the energy and variance of the approximate solutions with $Ra = 10^4$. The variance of the perturbed solutions indicates that they do not deviate much from the mean and therefore not much from each other. This seems to explain, in part, why the energy associated with these solutions is similar.

Interestingly, the energy associated with the unperturbed and mean computed solutions sit atop of one another; that is, the mean leads to a superior estimate than either member of the ensemble. It seems that the BV algorithm generated a positive/negative initial condition pair leading to two solutions whose average approximates the unperturbed solution well.

Figures 4 and 5 present $\gamma_{t^*}(t)$ and t_p for mean temperature and velocity approximations for $10^2 \leq Ra \leq 10^4$ and $\|(\chi_+ - \chi_-)(0)\| \leq \delta \leq 0.15$. The approximated effective Lyapunov exponent $\gamma_{t^*}(0)$ and t_p are negative for both velocity and temperature for all Rayleigh numbers indicating a predictable flow. However, $\gamma_{t^*}(t)$ changes sign for temperature and velocity at approximately $t = 0.11$ for $Ra = 10^4$ indicating a loss of predictability.

6. Conclusion. We presented two algorithms for calculating an ensemble of solutions to two laminar natural convection problems. These algorithms addressed the competition between ensemble size and resolution in simulations. In particular, both algorithms required the solution of a single matrix equation, at each time step, with multiple right hand sides. Stability and convergence were proven and numerical experiments were performed to illustrate these properties.

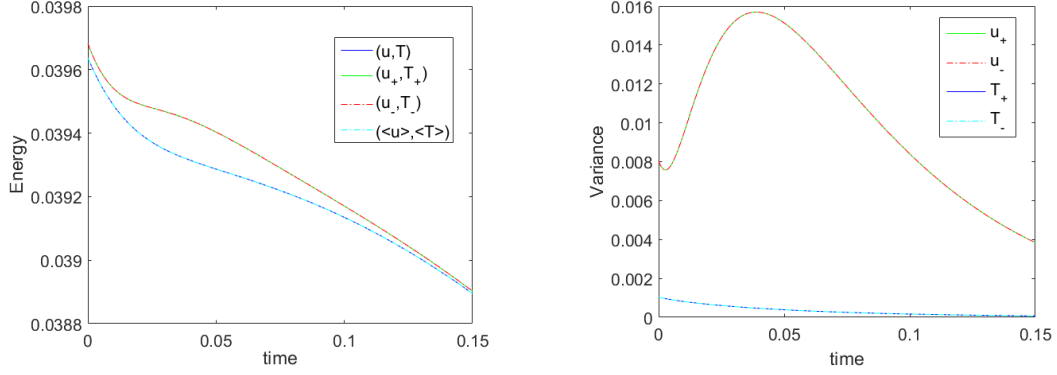


Fig. 3: Comparison of the energy in the system (left) and variance of each velocity and temperature ensemble member (right).

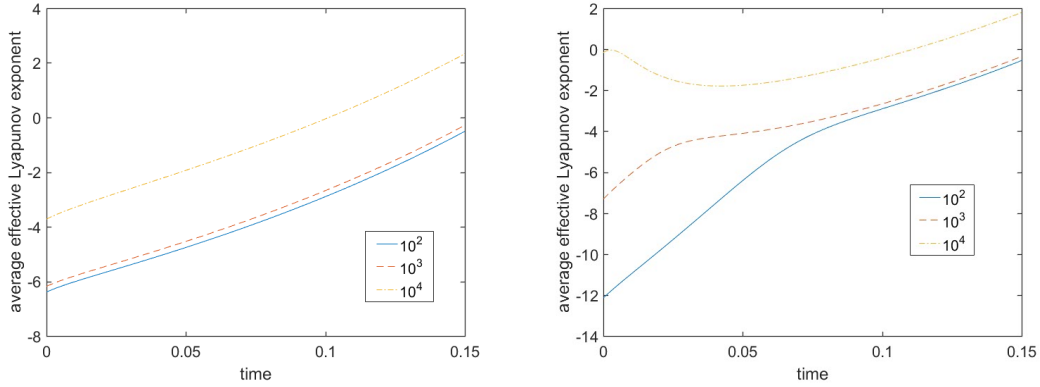


Fig. 4: Comparison of average effective Lyapunov exponent for temperature (left) and velocity (right).

Acknowledgments. The author J.A.F. is supported by the DoD SMART Scholarship. Moreover, the research herein was partially supported by NSF grants CBET 1609120 and DMS 1522267. Further, the authors would like to thank Dr. Nan Jiang for her input and discussion.

REFERENCES

- [1] A. Baïri, E. Zarco-Pernia, and J.-M. García de María, A review on natural convection in enclosures for engineering applications. The particular case of the parallelogrammic diode cavity. *Appl. Therm. Eng.*, 63:304-322, 2014.
- [2] G. Boffetta, A. Celani, A. Crisanti, and A. Vulpiani, Predictability in two-dimensional decaying turbulence. *Phys. Fluids*, 9:724-734, 1997.
- [3] J. Boland and W. Layton, An analysis of the finite element method for natural convection problems. *Numer. Methods Partial Differential Equations*, 2:115-126, 1990.
- [4] A. Cibik and S. Kaya, A projection-based stabilized finite element method for steady-state natural convection problem. *J. Math. Anal. Appl.*, 381:469-484, 2011.
- [5] A. Ern and J.-L. Guermond, *Theory and Practice of Finite Elements*. Springer-Verlag, New York, 2004.
- [6] N. Jiang and W. Layton, An Algorithm for Fast Calculation of Flow Ensembles. *Int. J. Uncertain. Quantif.*, 4:273-301, 2014.
- [7] B. Gebhart, Buoyancy induced fluid motions characteristic of applications in technology. *J. Fluids Eng.*, 101:5-28, 1979.
- [8] V. Girault and P. A. Raviart, *Finite Element Approximation of the Navier-Stokes Equations*. Springer, Berlin, 1979.
- [9] F. Hecht, New development in freefem++. *J. Numer. Math.*, 20:251-265, 2012.
- [10] J. G. Heywood and R. Rannacher, Finite-Element Approximation of the Nonstationary Navier-Stokes Problem Part IV: Error Analysis for Second-Order Time Discretization. *SIAM J. Numer. Anal.*, 27:353-384, 1990.
- [11] N. Jiang and W. Layton, Numerical analysis of two ensemble eddy viscosity numerical regularizations of fluid motion. *Numerical Methods for Partial Differential Equations*, 31:630-651, 2015.
- [12] E. Kalnay, *Atmospheric modeling, data assimilation and predictability*. Cambridge University Press, New York, 2003.

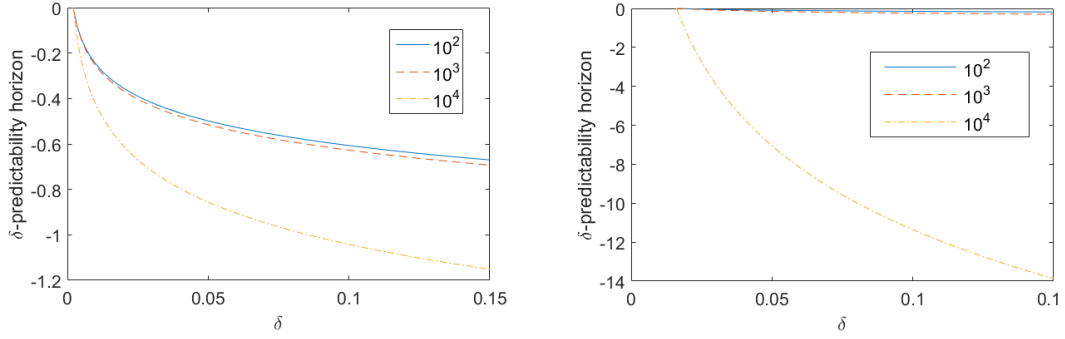


Fig. 5: Comparison of δ -predictability horizons for temperature (left) and velocity (right).

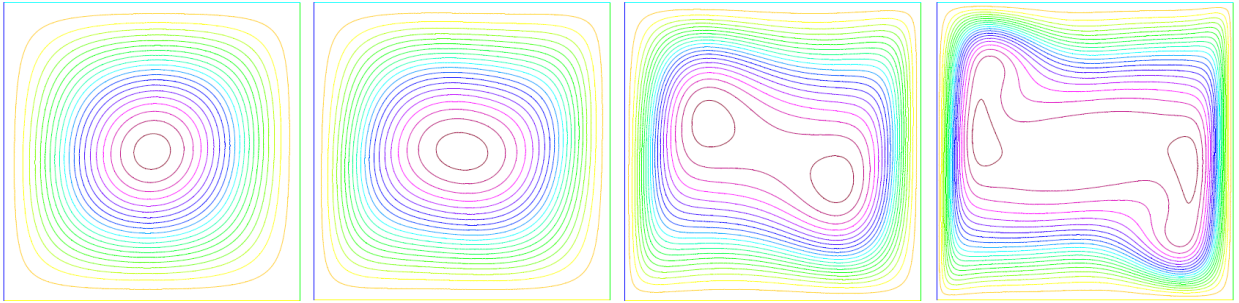


Fig. 6: Streamlines for $Ra = 10^3, 10^4, 10^5$, and 10^6 , from left to right, respectively.

- [13] W. Layton and L. Tobiska, A Two-Level Method with Backtracking for the Navier-Stokes Equations. SIAM J. Numer. Anal., 35:2035-2054, 1998.
- [14] P. Lermusiaux, Uncertainty estimation and prediction for interdisciplinary ocean dynamics. J. Comput. Phys., 217:860-877, 2006.
- [15] M. T. Manzari, An explicit finite element algorithm for convective heat transfer problems. Int. J. Numer. Methods Heat Fluid Flow, 9:860-877, 1999.
- [16] J. Marshall and F. Schott, Open-ocean convection: Observations, theory, and models. Rev. Geophys., 37:1-64, 1999.
- [17] S. Ostrach, Natural Convection in Enclosures. J. Heat Transfer, 110:1175-1190, 1988.
- [18] Z. Toth and E. Kalnay, Ensemble Forecasting at NMC: The Generation of Perturbations. Bull. Am. Meteorol. Soc., 74:2317-2330, 1993.
- [19] D. de Vahl Davis, Natural convection of air in a square cavity: A benchmark solution. Internat. J. Numer. Methods Fluids, 3:249-264, 1983.
- [20] D.C. Wan, B. S. V. Patnaik, and G. W. Wei, A new benchmark quality solution for the buoyancy-driven cavity by discrete singular convolution. Numer. Heat Transfer, 40:199-228, 2001.
- [21] Y. Yu, M. Zhao, T. Lee, N. Pestieau, W. Bo, J. Glimm, and J. W. Grove, Uncertainty quantification for chaotic computational fluid dynamics. J. Comput. Phys., 217:200-216, 2006.
- [22] Y. Zhang and Y. Hou, The Crank-Nicolson Extrapolation Stabilized Finite Element Method for Natural Convection Problem. Mathematical Problems in Engineering, 2014:1-22, 2014.

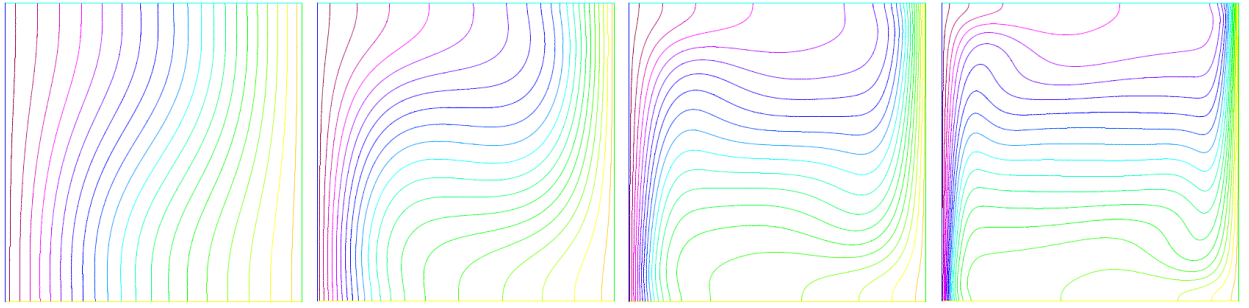


Fig. 7: Isotherms for $Ra = 10^3, 10^4, 10^5$, and 10^6 , from left to right, respectively.